European Journal of Medicinal Chemistry 171 (2019) 195–208

Contents lists available at ScienceDirect

European Journal of Medicinal Chemistry

journal homepage: http://www.elsevier.com/locate/ejmech

Research paper

Diphenyl ether derivatives occupy the expanded binding site of cyclohexanedione compounds at the colchicine site in tubulin by movement of the αT5 loop

Oskia Bueno [a], Marta Gargantilla [a], Juan Estévez-Gallego [b], Solange Martins [c], J. Fernando Díaz [b], María-José Camarasa [a], Sandra Liekens [c], María-Jesús Pérez-Pérez [a], Eva-María Priego [a, *]

[a] Instituto de Química Médica (IQM, CSIC), Juan de la Cierva 3, 28006, Madrid, Spain
[b] Centro de Investigaciones Biológicas (CIB,CSIC), Ramiro de Maeztu 9, 28040, Madrid, Spain
[c] Rega Institute for Medical Research, KU Leuven, Herestraat 49, B-3000, Leuven, Belgium

ARTICLE INFO

Article history:
Received 19 December 2018
Received in revised form
28 February 2019
Accepted 18 March 2019
Available online 21 March 2019

Keywords:
Colchicine domain
Structure-based design
Affinity maps
Diphenyl ethers

ABSTRACT

Microtubule targeting agents represent a very active arena in the development of anticancer agents. In particular, compounds binding at the colchicine site in tubulin are being deeply studied, and the structural information recently available on this binding site allows structure-directed design of new ligands. Structural comparison of our recently reported high resolution X-Ray structure of the cyclohexanedione derivative TUB075 bound to tubulin and the tubulin-DAMA-colchicine complex has revealed a conformational change in the αT5 loop. By a grid-based computational analysis of the tubulin-DAMA-colchicine binding site, we have identified a new favourable binding area in the colchicine-site that was unexplored by our lead TUB075. Thus, based on a structure-guided design, new cyclohexanedione derivatives have been synthesized and tested for tubulin binding and in cellular assays. As a result, we have identified diphenyl ether derivatives with IC_{50} values around 10–40 nM against three different tumor cell lines and affinity constants for tubulin similar to that of colchicine around $10^7\ M^{-1}$. As expected, they halted the cell cycle progression at G2/M phase at concentrations as low as 0.08 μM.

1. Introduction

Microtubules are highly dynamic polymers composed of αβ-tubulin heterodimers. These key components of the cytoskeleton of eukaryotic cells are involved in pivotal biological functions such as intracellular migration and transport, cell signalling, cell shape maintenance, cell motility and mitosis [1]. Their crucial role in cell division has made tubulin and microtubules important targets for several conditions, especially for cancer, and therefore antitubulin compounds represent the most successful class of antimitotic agents in cancer chemotherapy [2]. To date, several chemical classes of microtubule targeting agents (MTAs) are known, both from natural sources or synthetic derivatives [3,4].

At the cellular level, and according to their mechanism of action, MTAs can be divided as microtubule-stabilizing agents [5], i.e. placlitaxel (**1**) from the taxoid family, epothilone A (**2**) and laulimalilde (**3**) or as destabilizing agents like the vinca alkaloids such as vinblastine (**4**), colchicine (**5**) or combretastatins (**6, 7**), among others (Fig. 1) [3].

At the molecular level, MTAs bind to αβ-tubulin heterodimers at six different binding sites that are referred to as the taxane, colchicine, vinca, maytansine, laulimalide/peloruside and pironetin sites, all of which have been structurally characterized by high resolution X-ray crystallography and cryo-electron microscopy [6].

As recently reviewed [7], the mechanism of action of MTAs goes far beyond than acting as antimitotic agents. Since microtubule structure and function are crucial for cell motility and shape, compounds affecting microtubules dynamics may lead to anti-metastatic and antiangiogenic effects [8,9]. Tubulin destabilization has also been linked to vascular disruption so that morphological changes in the vascular endothelial cells increase vascular permeability leading to blood flow occlusion. This is particularly relevant

* Corresponding author. Instituto de Química Médica (CSIC), c/ Juan de la Cierva 3, E-28006, Madrid, Spain. Tel.: +34915680040; fax: +34915644853.
E-mail address: empriego@iqm.csic.es (E.-M. Priego).

https://doi.org/10.1016/j.ejmech.2019.03.045
0223-5234/

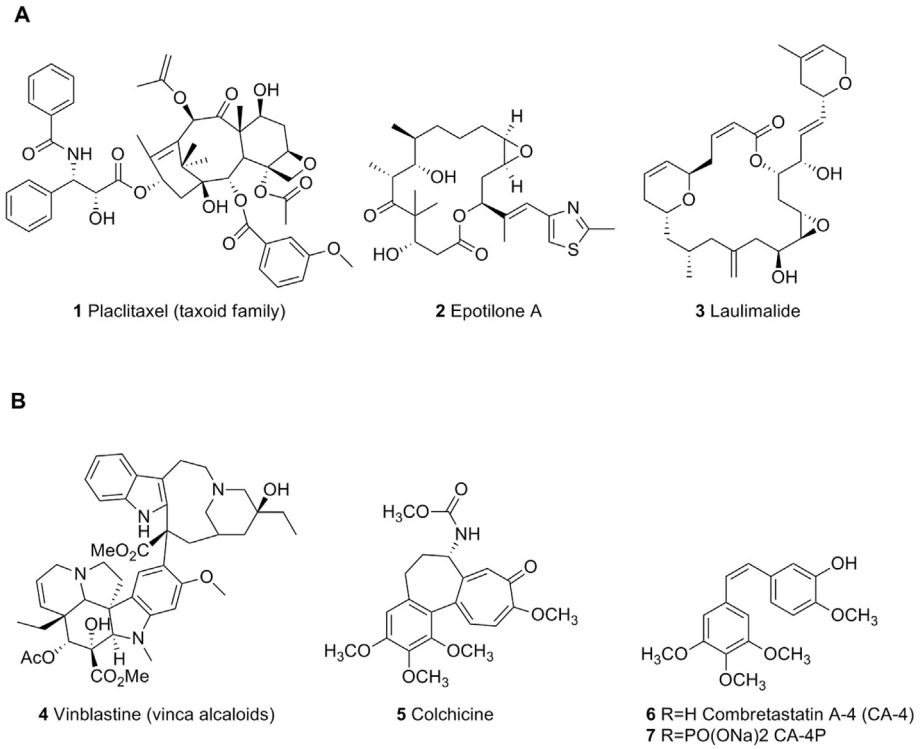

Fig. 1. Chemical structures of selected microtubule-stabilizing (A) and microtubule-destabilizing (B) agents.

for tumor vessels because of their significant differences with physiological vessels (i.e increased vascular permeability) [10]. Thus, treatment with vascular disrupting agents (VDAs) has been proposed as an interesting antitumor approach leading to vascular shutdown and tumor necrosis, although the outer rim of the tumor remains unaffected, which support the use of VDAs combined with other anticancer treatments [11]. Among VDAs, destabilizing tubulin-colchicine-site binders have been extensively studied [12,13].

The colchicine site is a hydrophobic pocket located near the intra-dimer interface between the α and β tubulin subunits [14]. Based on the structural information available, two distinct binding modes of colchicine-site ligands have been characterized [15], with compounds that bind deeper in the β subunit such as TN-16 (**8**), and compounds that bind closer to the interface between α and β subunits of a tubulin dimer, the prototype being DAMA-colchicine (**9**) (Fig. 2A). We have recently reported the high resolution X-Ray structure of the cyclohexanedione derivative TUB075 (**10**, Fig. 2A) bound to αβ-tubulin, compound that binds mostly at the β-subunit, similar to TN-16 [16]. Superposition of the crystal structures of tubulin-DAMA-colchicine and tubulin-TUB075 complexes revealed a significant conformational change of the α-T5 loop (Fig. 2B). This loop closed the TUB075 binding site in the tubulin-TUB075 complex while it was flipped out in the DAMA-colchicine structure. Based on this loop movement, it could be argued that DAMA-colchicine makes uses of binding/affinity areas of the binding domain that are not accessible for TUB075. Therefore, we have dissected the binding mode of DAMA-colchicine with different probes, using the computational tool cGRILL [17]. By unravelling new potential affinity areas with cGRILL, structure-guided design of TUB075 based derivatives has been carried out leading to the synthesis of new cyclohexanedione derivatives with a distal diphenyl ether moiety. In addition, the tubulin binding and the antiproliferative evaluation of the new compounds have been accomplished.

2. Results and discussion

2.1. Affinity maps of the DAMA-colchicine-tubulin complex for the design of new ligands

To identify new favourable binding areas unexplored by TUB075 at the colchicine domain, the corresponding affinity maps on the tubulin-DAMA-colchicine complex (PDB ID: 1sa0) [14] were generated by means of the computational tool cGRILL and the lipophilic probe (CH3+) [17,18]. As shown in Fig. 3A, three well-defined affinity areas encircle DAMA-colchicine: area 1, located inside the β-subunit; area 2, covering the lower part of the trimethoxyphenyl ring of DAMA-colchicine (ring A); and area 3, where the tropone ring of DAMA-colchicine (ring C) is located. When TUB075 was superimposed onto this affinity maps, it became clear that areas 1 and 2 were already occupied by rings A, B and D of TUB75, whereas area 3 was scarcely explored by TUB075 although the ethoxy group seemed to point towards it. Given the shape and the lipophilic character of this unexplored area, we reasoned that, keeping the oxygen atom as bridge, the incorporation of an additional aromatic ring (named ring E) linked to ring D, could fulfil this affinity region, thus resulting in new diphenyl ether derivatives (Fig. 3B).

2.2. Chemistry

The synthesis of the required 2-phenoxyanilines (**14a-j**) was carried out in a two-step process involving the nucleophilic aromatic substitution (S_NAr) of 1-fluoro-2-nitrobenzene (**11**) with differently functionalized phenols at positions 3 and/or 4, followed by reduction of the nitro derivatives (Scheme 1). Thus, 2-nitrodiphenyl ethers (**12a-e**) were prepared via a modified

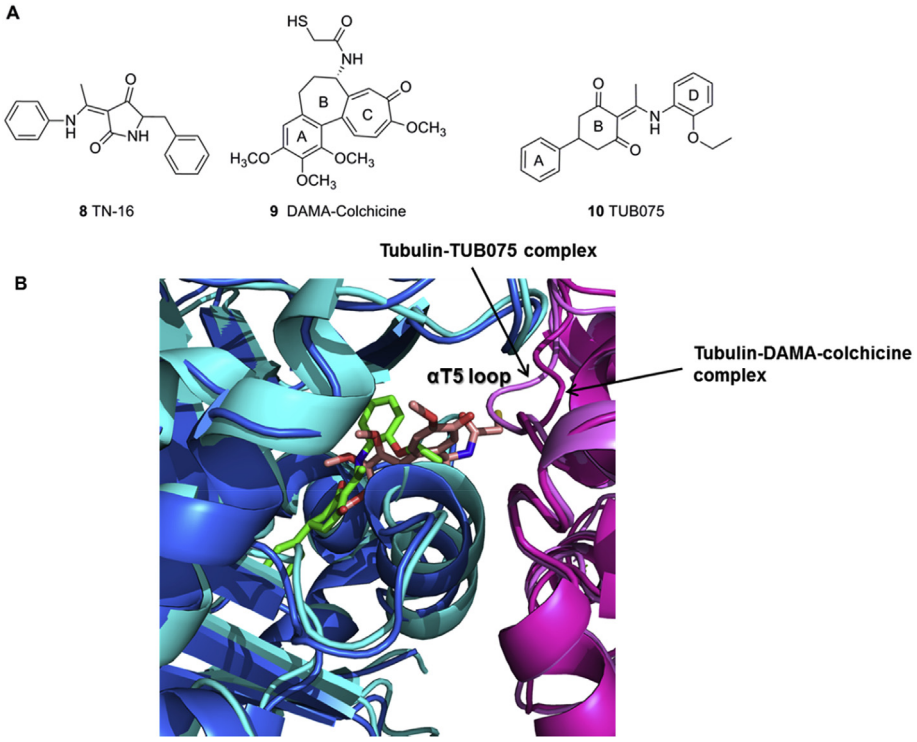

Fig. 2. (A) Chemical structures of TN-16, DAMA-colchicine and TUB075. (B) Movement of the α-T5 loop. Superposition of tubulin-DAMA-colchicine complex (α-tubulin in magenta, β-tubulin in blue marine and DAMA-colchicine in orange) with TUB075-tubulin complex (α-tubulin in light pink, β-tubulin in cyan and TUB075 in green). (For interpretation of the references to color in this figure legend, the reader is referred to the Web version of this article.)

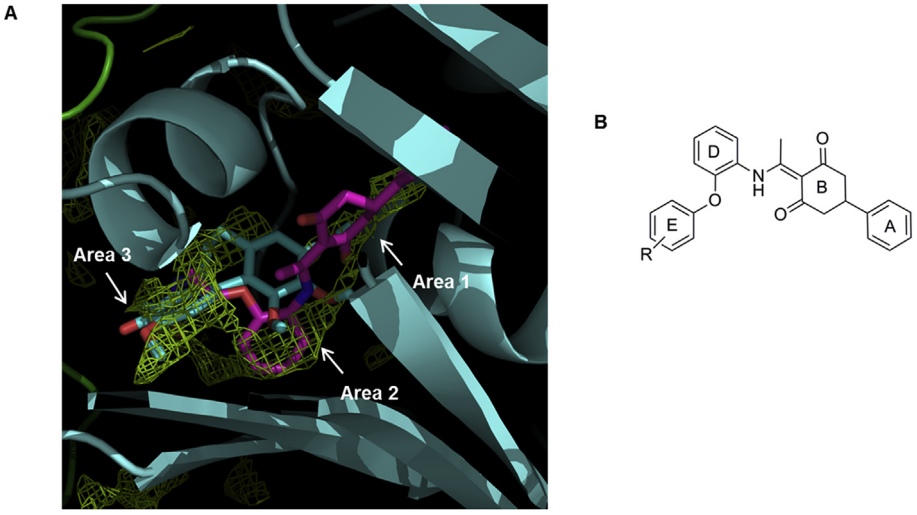

Fig. 3. (A) Affinity maps generated with the lipophilic probe CH3+ (green grid) onto tubulin-DAMA-colchicine (cyan sticks) complex and its superposition with TUB075 (magenta sticks). (B) General structure of the new diphenyl ether derivatives. (For interpretation of the references to color in this figure legend, the reader is referred to the Web version of this article.)

described procedure [19]. Reaction of 1-fluoro-2-nitrobenzene (**11**) with 3-fluoro (**12a**), 4-chloro (**12b**), 3-methoxy (**12c**), 4-methoxy (**12d**) and 3,4-dimethoxy (**12e**) phenols in the presence of Cs_2CO_3 in acetonitrile at 80 °C afforded the corresponding nitro derivatives (**13a-e**) in excellent yields (88–99%). Under the same conditions, the NH-Boc protected phenols (**12f-h**) [20–22] and 4-hydroxyacetophenone (**12i**) reacted with **11** to yield the corresponding nitro derivatives **13f-i**. Finally, catalytic hydrogenation of the halogenated compounds **13a-b** in the presence of Pt/S or in the presence of Pd/C for the rest of the compounds (**13c-i**), yielded the corresponding 2-phenoxyanilines **14a-i**. Aniline **14i** was obtained in 42% yield together with compound **14j** by partial reduction of the carbonyl group.

As shown in Scheme 2, reaction of 2-acetyl-5-phenylcyclohexane-1,3-dione (**15**) [23] with the synthesized anilines **14a-j** in toluene at 110 °C in the presence of 4 Å molecular sieves [24] led to the final compounds **16a-j** in moderate to good yields. For comparative purposes, the unsubstituted derivative at

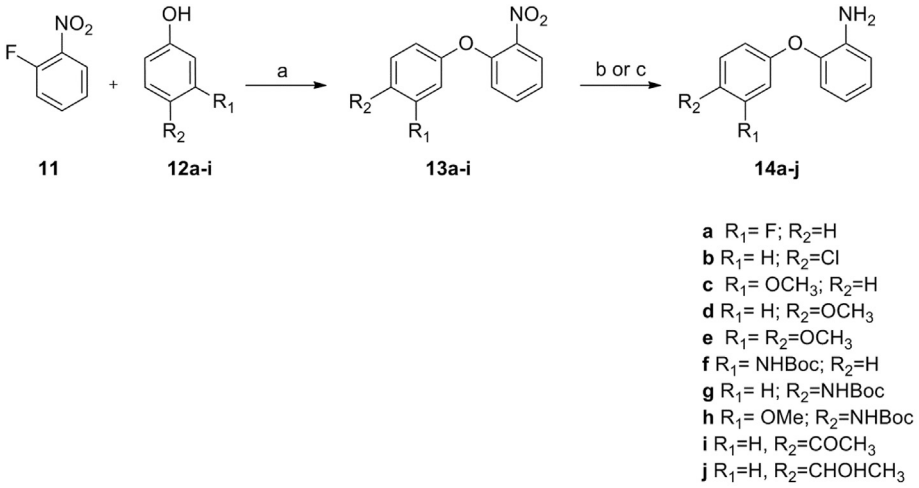

Scheme 1. Reagents and conditions: (a) Cs_2CO_3, CH_3CN, 80 °C, 2–5 h, 88–99% yields; (b) for **13a,b**: H_2, Pt/S 5%, AcOEt, 30 psi, rt, 2 h, 74–84% yields; (c) for **13e-i**: H_2, Pd/C 10%, AcOEt, 30 psi, rt, 1–4 h, 42–99% yields.

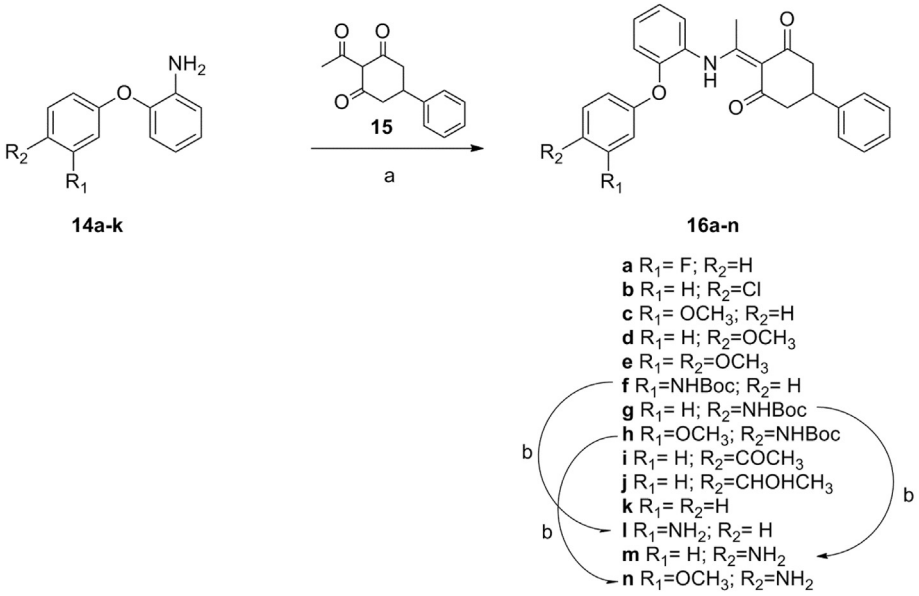

Scheme 2. Reagents and conditions: (a) Toluene, molecular sieves 4 Å, pressure tube, 110 °C, 16 h, 28–99% yields; (b) TFA, CH_2Cl_2, rt, 20 min-1 h, 88–99% yields.

ring E (**16k**) was also synthesized from the commercially available 2-phenoxyaniline (**14k**). Finally, treatment of *N*-Boc derivatives **16f-h** with TFA yielded the free amino cyclohexanediones **16l-n**.

2.3. Antiproliferative activity

The synthesized diphenyl ether derivatives were evaluated for their anti-proliferative activity in three different cancer cell lines [mouse leukemia (L1210), human lymphoblastic leukemia (CEM) and human cervical carcinoma (HeLa) cells] and one endothelial cell line [human microvascular endothelial cells (HMEC-1)]. Data are collected in Table 1 and expressed as IC_{50} (50% inhibitory concentration) representing the concentration at which the compounds reduce cell proliferation by 50%. Colchicine (**5**) and CA-4P (**7**) are included as reference compounds while data from our previous hit TUB075 (**10**) is included for comparative purposes [16].

The data collected in Table 1 revealed that the introduction of an extra aromatic ring (ring E) in the structure of TUB075 led to highly potent antiproliferative compounds with IC_{50} in the sub-micromolar range in all the cells lines tested. Thus, compound **16k** with an unsubstituted phenyl ring provides IC_{50} values similar or slightly better than those of the reference compound TUB075. Incorporation of halogens at this phenyl ring, either a fluor at position 3 (**16a**) or a chlorine at position 4 (**16b**) did not improve the antiproliferative activity. On the other hand, introduction of a methoxy group at position 3, 4 or both (derivatives **16c**, **16d** and **16e**, respectively) led to an improvement in the antiproliferative activities with IC_{50} values ranging from 0.04 to 0.16 μM, being the 3-OMe derivative **16c** the most potent among them. Interestingly, compounds with amino groups in positions 3 or 4 of ring E, (**16l** and **16m**, respectively) also provided very interesting antiproliferative activities, with IC_{50} values ranging between 0.037 and 0.082 μM. Finally, the double substituted compound **16n**, with a methoxy group at 3 and an amino group at 4, provided excellent antiproliferative activity against all the cell lines tested with IC_{50} values between 0.012 and 0.033 μM.

Table 1
Anti-proliferative activity of the diphenylether derivatives (**16a-n**) in endothelial and tumor cell lines.

Comp.	Tumor cells IC_{50} (μM)[a]			Endothelial cells IC_{50} (μM)[a]
	L1210	CEM	HeLa	HMEC-1
TUB075 (10)	0.19 ± 0.05	0.19 ± 0.01	0.18 ± 0.0	0.10 ± 0.02
16a	0.33 ± 0.10	0.17 ± 0.06	0.55 ± 0.30	0.36 ± 0.036
16b	0.25 ± 0.01	0.19 ± 0.02	0.50 ± 0.40	0.26 ± 0.030
16c	0.058 ± 0.014	0.041 ± 0.007	0.093 ± 0.022	0.059 ± 0.001
16d	0.14 ± 0.08	0.12 ± 0.02	0.16 ± 0.03	0.083 ± 0.004
16e	0.065 ± 0.003	0.16 ± 0.00	0.054 ± 0.014	0.14 ± 0.03
16i	0.19 ± 0.02	0.22 ± 0.01	0.13 ± 0.01	0.18 ± 0.01
16j	0.058 ± 0.01	0.12 ± 0.00	0.075 ± 0.012	0.14 ± 0.04
16k	0.086 ± 0,003	0.17 ± 0.01	0.079 ± 0.031	0.16 ± 0.04
16l	0.053 ± 0.006	0.042 ± 0.001	0.082 ± 0.063	0.041 ± 0.008
16m	0.040 ± 0.002	0.037 ± 0.005	0.039 ± 0.000	0.047 ± 0.019
16n	0.026 ± 0.007	0.012 ± 0.008	0.033 ± 0.000	0.029 ± 0.003
Colchicine (5)	0.010 ± 0.0006	0.013 ± 0.0004	0.0087 ± 0.0001	0.0038 ± 0.0011
CA-4P (7)	0.013 ± 0.0023	0.011 ± 0.001	0.013 ± 0.001	0.0029 ± 0.0001

[a] IC_{50} (50% inhibitory concentration) is given as the mean ±SD of three independent experiments.

2.4. Tubulin binding

In order to corroborate whether the antiproliferative activity of these diarylethers was derived from their interaction with tubulin, the effect on dimeric tubulin polymerization into microtubules was tested in a turbidimetric assay including podophylotoxin as control. As shown in Fig. 4, at the tested concentration all compounds displayed a destabilizing effect of tubulin polymerization similar to that of podophylotoxin.

In addition, binding affinities for all final compounds to tubulin were determined by a competition experiment with R-PT as previously described [16,25]. The data obtained are collected in Table 2. All the compounds showed a remarkable affinity for tubulin, with K_b values ranging from 10^6 to $10^7\ M^{-1}$. The best K_b values correspond to compounds **16c** ($K_b = 15.65 \times 10^6$), **16m** ($K_b = 11.75 \times 10^6$ T) and **16n** ($K_b = 18.05 \pm x\ 10^6$), and are similar to that of colchicine ($K_b = 11.6 \times 10^6\ M^{-1}$). Interestingly, these compounds were also among the ones that provided better antiproliferative activity in cell culture.

2.5. Cell cycle experiments

Compounds **16m** and **16n**, two of the most active derivatives in this series, were selected to further investigate their antimitotic behaviour due to cell cycle arrest. Thus, we performed cell cycle analysis on HMEC-1 cells at different concentrations (0.016, 0.08 and 0.4 μM) for 24 h. As shown in Fig. 5, control (untreated) cells showed the typical distribution pattern of proliferating cells while treatment with 0.08 or 0.4 μM of **16m** (Fig. 5A) or **16n** (Fig. 6B) caused an accumulation in G2/M phase, indicating antimitotic activity. Cell cycle analysis has also been performed with compounds **16m** and **16n** in HeLa cells, using colchicine as reference compound, with similar results (Fig. S1).

2.6. Vascular disrupting activity

It is well established that compounds binding at the colchicine site in tubulin are able to destroy the vasculature network formed by endothelial cells. HMEC-1 cells were seeded on top of matrigel and after 3 h a network of endothelial cells is visible (control). Then derivatives **16m** or **16n** were added at different concentrations (2, 0.4 and 0.08 μM). As can be seen in Fig. 6 the addition of the compounds led to vascular disrupting activity in a dose-dependent manner, being visible still at 0.4 μM.

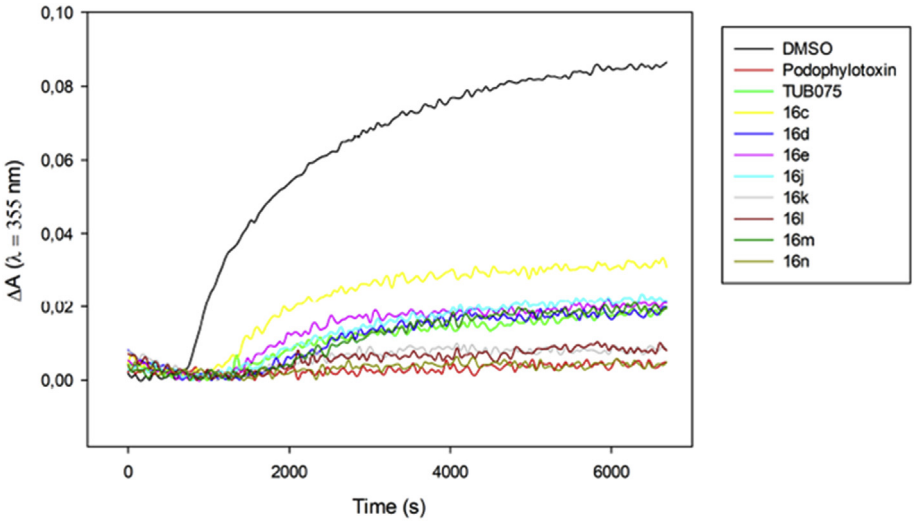

Fig. 4. Time course of tubulin polymerization at 37 °C measured by 350 nm turbidimetry. Tubulin concentration: 25 μM, compounds **16c-n** 30 μM.

Table 2
Binding constants for αβ-tubulin.

Comp	Kb (M^{-1})
Colchicine (**5**)	11.6×10^6 [a] [26]
Podophyllotoxin	1.8×10^6 [a] [27]
R-PT	3.2×10^6 [25]
TUB075 (**10**)	$(13 \pm 2) \times 10^6$ [a]
16c	$(15.65 \pm 5.55) \times 10^6$ [a]
16d	$(5.23 \pm 0.24) \times 10^6$ [a]
16e	$(2.24 \pm 0.33) \times 10^6$ [a]
16j	$(3.13 \pm 0.11) \times 10^6$ [a]
16k	$(6.46 \pm 0.91) \times 10^6$ [a]
16l	$(5.56 \pm 1.25) \times 10^6$ [a]
16m	$(11.75 \pm 2.95) \times 10^6$ [a]
16n	$(18.05 \pm 8.05) \times 10^6$ [a]

[b]Mean value of three experiments ± StdError
[a] At 25 °C.

2.7. Docking studies

To gain a better understanding on the potency and the binding mode of the most potent compound **16n** to tubulin, a docking study was performed using the coordinates of the TUB075-tubulin complex (pdb id: 6KFJ) as template. The best docking pose of **16n** into the colchicine domain in tubulin (Fig. 7A) showed that regions A, B, C and D of **16n** (showed in cyan sticks in Fig. 7A) occupies the same pocket as TUB075 (represented in nude sticks) sharing also the same orientation, which allows **16n** to keep the crucial hydrogen-bond interaction with Glu200, as reported for TUB075. Regarding the new ring E, it is directed towards the interface between α and β subunits and the amino group present in this ring E is at hydrogen bond distance (2.5 Å) to the backbone carbonyl of Thrα179, which is located in the αT5-loop. Moreover, superposition of this predicted binding mode of **16n** and the tubulin-DAMA-colchicine complex (Fig. 7B) showed that ring E is overlapping with the tropone ring of DAMA-colchicine, thus confirming our rational design of these new derivatives.

3. Conclusions

Taken advantage of the high resolution X-ray structure of the cyclohexanedione derivative TUB075 bound to αβ-tubulin, a detailed structural comparison with the tubulin-DAMA-colchicine complex has revealed a significant conformational change of the αT5 loop, that closed the TUB075 binding site in the tubulin-TUB075 complex while it was flipped out in the DAMA-colchicine structure. Applying the computational tool cGRILL to the tubulin-DAMA-colchicine complex, and using CH_3 probe, a new potential binding area barely explored by TUB075 at the colchicine site was identified. Thus, a series of diphenyl ether derivatives has been synthesized and tested. The introduction of an extra aromatic ring in the structure of TUB075 has led to highly potent antiproliferative compounds, being compound **16n**, with a methoxy group at 3 and an amino group at 4, the most active among them, with IC_{50} values between 0.012 and 0.033 μM, and a tubulin binding constant value of $18.05 \pm x \ 10^6 \ M^{-1}$, similar to that of colchicine ($K_b = 11.6 \times 10^6 \ M^{-1}$). Moreover, additional biological studies have showed that compounds **16n** and **16m** held antimitotic activity by an accumulation of cells in G2/M phase and a dose-dependent vascular disrupting activity in the low micromolar range.

4. Experimental

4.1. Chemistry procedures

Melting points were obtained on a Reichert-Jung Kofler apparatus and are uncorrected. The elemental analysis was performed with a Heraeus CHN-O-RAPID instrument. The elemental compositions of the compounds agreed to within ±0.4% of the calculated values.

Electrospray mass spectra were measured on a quadrupole mass spectrometer equipped with an electrospray source (Hewlett-Packard, LC/MS HP 1100).

^1H and ^{13}C NMR spectra were recorded on a Varian INNOVA 300 operating at 299 MHz (^1H) and 75 MHz (^{13}C), respectively, a Varian INNOVA-400 operating at 399 MHZ (^1H) and 99 MHz (^{13}C), respectively, and a VARIAN SYSTEM-500 operating a 499 MHz (^1H) and 125 MHz (^{13}C), respectively. Monodimensional ^1H and ^{13}C spectra were obtained using standard conditions. 2D inverse proton detected heteronuclear one-bond shift correlation spectra were obtained using the Pulsed Field Gradient HSQC pulse sequence. Data were collected in a 2048 × 512 matrix with a spectral width of 3460 Hz in the proton domain and 22,500 Hz in the carbon domain, and processed in a 2048 × 1024 matrix. The experiment was optimized for one bond heteronuclear coupling constant of 150 Hz. 2D inverse proton detected heteronuclear long range shift correlation spectra were obtained using the Pulsed Field Gradient HMBC pulse sequence. The HMBC experiment was acquired in the same conditions that HSQC experiment and optimized for long range coupling constants of 7 Hz.

Analytical TLC was performed on silica gel 60 F_{254} (Merck)

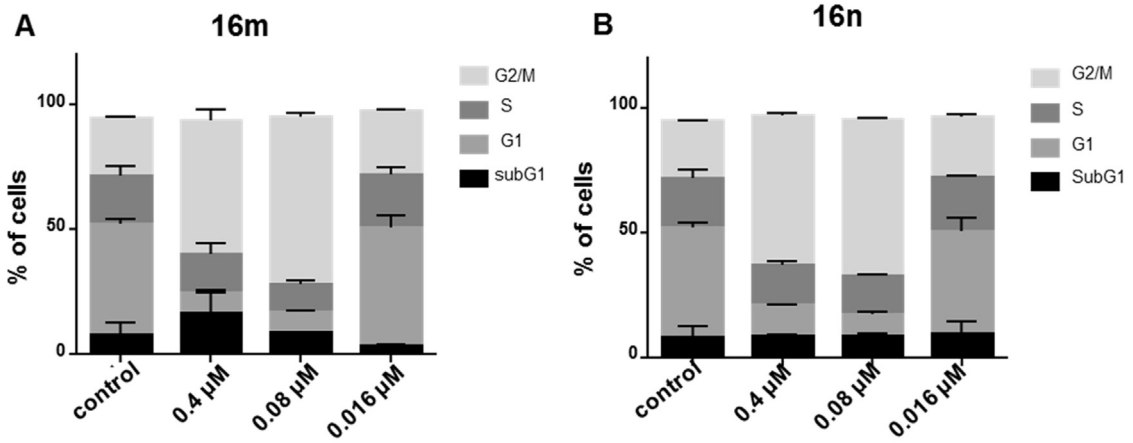

Fig. 5. Flow cytometric analysis of cell cycle distribution of HMEC-1 cells treated for 24 h with different concentrations of **16m** (a), **16n** (b).

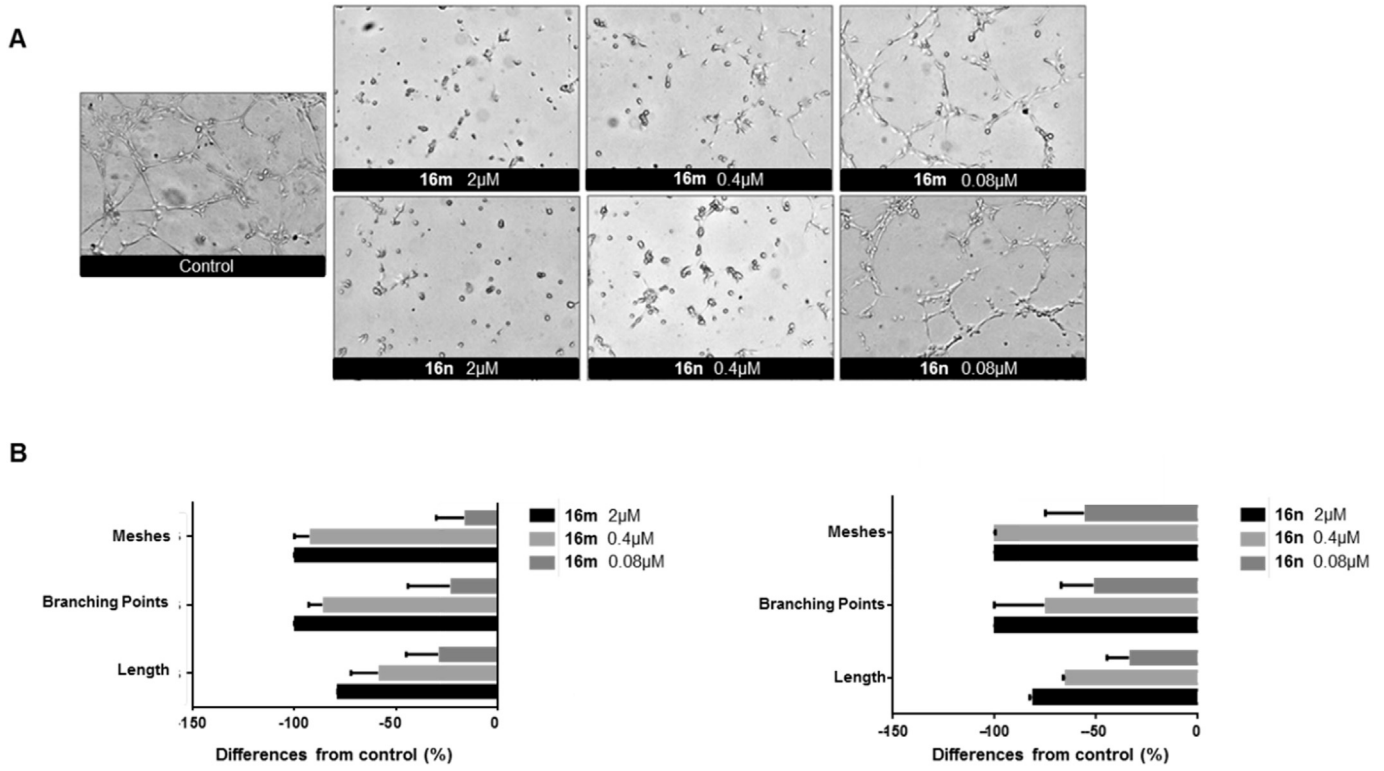

Fig. 6. (A) Vascular disrupting effects of **16m** and **16n**. (B) After 90 min the number of meshes, branching points and length of the tubes were quantified using Image J analysis.

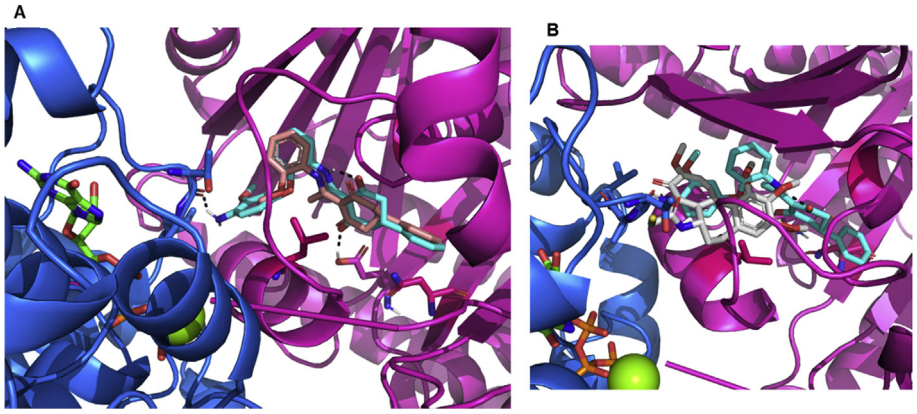

Fig. 7. (A) Predicted binding mode of **16n** (cyan) in the colchicine domain of αβ-tubulin (α-subunit in blue and β subunit in magenta) and overlap with TUB075 (nude). Dashed lines indicate hydrogen bonds and selected interaction residues are shown in sticks and labelled. (B) Superposition of **16n** (cyan) and DAMA-colchicine (white). (For interpretation of the references to color in this figure legend, the reader is referred to the Web version of this article.)

precoated plates (0.2 mm). Spots were detected under UV light (254 nm) and/or charring with ninhydrin or phosphomolibdic acid.

Separations on silica gel were performed by preparative centrifugal circular thin-layer chromatography (CCTLC) on a Chromatotron^{R} (Kiesegel 60 PF_{254} gipshaltig (Merck)), with layer thickness of 1 and 2 mm and flow rate of 4 or 8 mL/min, respectively. Flash column chromatography was performed in a Biotage Horizon instrument.

Microwave reactions were performed using the Biotage Initiator 2.0 single-mode cavity instrument from Biotage (Uppsala). Experiments were carried out in sealed microwave process vials utilizing the standard absorbance level (400 W maximum power). The temperature was measured with an IR sensor on the outside of the reaction vessel.

4.1.1. General procedure [19] for the synthesis of 2-nitrodiphenyl ethers (general procedure A)

To a mixture of Cs_2CO_3 (1.0 mmol) and the substituted phenol (1.2 mmol) in anhydrous acetonitrile (2.5 mL/mmol), 1-fluoro-2-nitrobenzene (**11**) (1.0 mmol) was added dropwise while stirring under argon. After 2–5 h at 80 °C, water (20 mL) and sat. aq. $NaHCO_3$ solution (20 mL) was added and the mixture was extracted with ethyl acetate. The organic layer was dried over Na_2SO_4, concentrated, and purified by flash chromatography (hexane/ethyl acetate).

*4.1.1.1. 1-(4-Fluorophenoxy)-2-nitrobenzene (**13a**).* Following the general procedure A, to a mixture of Cs_2CO_3 (482 mg, 1.48 mmol) and 3-fluorophenol (**12a**) (162 μL, 1.70 mmol) in CH_3CN (3.6 mL), 1-fluoro-2-nitrobenzene (**11**) (156 μL, 1.48 mmol) was added. After 4 h at 80 °C, the residue was worked up and purified by flash chromatography (hexane/ethyl acetate, 10:1) to yield 310 mg (90%) of **13a** as a yellow oil. ^{1}H NMR (DMSO-d_6, 300 MHz): δ 6.88 (dd, J = 8.3, 2.4 Hz, 1H, Ar), 7.00 (m, 1H, Ar), 7.06 (dd, J = 8.5, 2.3 Hz, 1H, Ar), 7.27 (dd, J = 8.3, 1.2 Hz, 1H, Ar), 7.37–7.53 (m, 2H, Ar), 7.74 (m, 1H, Ar), 8.10 (dd, J = 8.2, 1.7 Hz, 1H, Ar). MS (ES, positive mode): 234 $(M + H)^+$. ^{1}H NMR data are similar to those previously described [28].

*4.1.1.2. 1-(4-Chlorophenoxy)-2-nitrobenzene (**13b**).* Following the general procedure A, to a mixture of Cs_2CO_3 (463 mg, 1.42 mmol) and 4-chlorophenol (**12b**) (167 μL, 1.70 mmol) in CH_3CN (3.6 mL), 1-fluoro-2-nitrobenzene (**11**) (149 μL, 1.42 mmol) was added. After 2 h at 80 °C, the residue was worked up and purified by flash chromatography (hexane/ethyl acetate 10:1) to yield 864 mg (99%) of **13b** as a yellow oil. ^{1}H NMR (DMSO-d_6, 300 MHz): δ 7.00–7.14 (m, 2H, Ar), 7.22 (dd, J = 8.4, 1.2 Hz, 1H, Ar), 7.41 (m, 1H, Ar), 7.45–7.52 (m, 2H, Ar), 7.72 (m, 1H, Ar), 8.09 (dd, J = 8.1, 1.7 Hz, 1H, Ar). ^{1}H NMR data are similar to those previously described [28].

*4.1.1.3. 1-(3-Methoxyphenoxy)-2-nitrobenzene (**13c**).* Following the general procedure A, to a mixture of Cs_2CO_3 (925 mg, 2.84 mmol) and 3-methoxyphenol (**12c**) (373 μL, 3.40 mmol) in CH_3CN (7.1 mL), 1-fluoro-2-nitrobenzene (**11**) (299 μL, 2.84 mmol) was added. After 3 h at 80 °C, the residue was worked up and purified by flash chromatography (hexane/ethyl acetate, 5:1) to yield 615 mg (88%) of **13c** as a yellow oil. ^{1}H NMR (DMSO-d_6, 400 MHz): δ 3.75 (s, 3H, CH_3), 6.59 (ddd, J = 8.2, 2.3, 0.8 Hz, 1H, Ar), 6.67 (t, J = 2.4 Hz, 1H, Ar), 6.79 (ddd, J = 8.4, 2.4, 0.8 Hz, 1H, Ar), 7.16 (dd, J = 8.4, 1.2 Hz, 1H, Ar), 7.32 (t, J = 8.2 Hz, 1H, Ar), 7.37 (ddd, J = 8.4, 7.4, 1.2 Hz, 1H, Ar), 7.69 (ddd, J = 8.3, 7.4, 1.7 Hz, 1H, Ar), 8.06 (dd, J = 8.1, 1.7 Hz, 1H, Ar). MS (ES, positive mode): 246 $(M + H)^+$.^{1}H NMR data are similar to those previously described [28].

*4.1.1.4. 1-(4-Methoxyphenoxy)-2-nitrobenzene (**13d**).* Following the general procedure A, to a mixture of Cs_2CO_3 (1.15 g, 3.54 mmol) and 4-methoxyphenol (**12d**) (528 mg, 4.25 mmol) in CH_3CN (9 mL), 1-fluoro-2-nitrobenzene (**11**) (374 μL, 3.54 mmol) was added dropwise while stirring under argon. After 3 h at 80 °C, the residue was worked up and purified by flash chromatography (hexane/ethyl acetate 10:1) to yield 864 mg (99%) of **13d** as a yellow solid. Mp 76–78 °C (lit [29] 75–76.5 °C); ^{1}H NMR (DMSO-d_6, 300 MHz): δ 3.76 (s, 3H, CH_3), 6.96–7.03 (m, 3H, Ar), 7.04–7.12 (m, 2H, Ar), 7.28 (m, 1H, Ar), 7.63 (m, 1H, Ar), 8.02 (dd, J = 8.1, 1.7 Hz, 1H, Ar). MS (ES, positive mode): 246 $(M + H)^+$. ^{1}H NMR data are similar to those previously described [19].

*4.1.1.5. 1,2-Dimethoxy-4-(2-nitrophenoxy)benzene (**13e**).* Following the general procedure A, to a mixture of Cs_2CO_3 (925 mg, 2.84 mmol) and 3,4-dimethoxyphenol (**12e**) (525 mg, 3.40 mmol) in CH_3CN (7.1 mL), 1-fluoro-2-nitrobenzene (**11**) (299 μL, 2.84 mmol) was added. After 5 h at 80 °C, the residue was worked up and purified by flash chromatography (hexane/ethyl acetate, 10:1) to yield 767 mg (97%) of **13e** as a yellow oil. ^{1}H NMR (DMSO-d_6, 400 MHz): δ 3.74 (s, 3H, CH_3), 3.76 (s, 3H, CH_3), 6.61 (dd, J = 8.7, 2.8 Hz, 1H, Ar), 6.85 (d, J = 2.8 Hz, 1H, Ar), 6.97–7.02 (m, 2H, Ar), 7.27 (ddd, J = 8.2, 7.4, 1.2 Hz, 1H, Ar), 7.63 (ddd, J = 8.5, 7.4, 1.7 Hz, 1H, Ar), 8.02 (dd, J = 8.1, 1.7 Hz, 1H, Ar). MS (ES, positive mode): 276 $(M + H)^+$. ^{1}H NMR data are similar to those previously described [19].

*4.1.1.6. tert-Butyl (3-(2-nitrophenoxy)phenyl)carbamate (**13f**).* Following the general procedure A, to a mixture of Cs_2CO_3 (694 mg, 2.13 mmol) and *tert*-butyl (3-hydroxyphenyl)carbamate (**12f**) [20] (534 mg, 2.55 mmol) in CH_3CN (5.3 mL), 1-fluoro-2-nitrobenzene (**11**) (224 μL, 2.13 mmol) was added dropwise while stirring under argon. After 4 h at 80 °C, the residue was worked up and purified by flash chromatography (hexane/ethyl acetate, 4:1) to yield 650 mg (92%) of **13f** as a yellow oil. **^{1}H NMR** (DMSO-d_6, 400 MHz): δ 1.44 (s, 9H, $(CH_3)_3$), 6.64 (ddd, J = 7.8, 2.3, 1.4 Hz, 1H, Ar), 7.15 (dd, J = 8.4, 1.2 Hz, 1H, Ar), 7.22–7.31 (m, 3H, Ar), 7.36 (ddd, J = 8.3, 7.5, 1.2 Hz, 1H, Ar), 7.69 (ddd, J = 8.2, 7.4, 1.7 Hz, Ar), 8.06 (dd, J = 8.2, 1.7 Hz, 1H, Ar), 9.51 (br s, 1H, NH). MS (ES, positive mode): 331 $(M + H)^+$, 661 $(2\ M + H)^+$.

*4.1.1.7. tert-Butyl (4-(2-nitrophenoxy)phenyl)carbamate (**13g**).* Following the general procedure A, to a mixture of Cs_2CO_3 (436 mg, 1.34 mmol) and *tert*-butyl(4-hydroxyphenyl)carbamate (**12g**) [21] (337 mg, 1.61 mmol) in CH_3CN (3.5 mL), 1-fluoro-2-nitrobenzene (**11**) (141 μL, 1.34 mmol) was added dropwise while stirring under argon. After 3 h at 80 °C, the residue was worked up and purified by flash chromatography (hexane/ethyl acetate, 4:1) to yield 512 mg (96%) of **13g** as yellow oil. ^{1}H NMR (DMSO-d_6, 400 MHz): δ 1.47 (s, 9H, $(CH_3)_3$), 6.99–7.05 (m, 3H, Ar), 7.29 (ddd, J = 8.3, 7.4, 1.2 Hz, 1H, Ar), 7.45–7.53 (m, 2H, Ar), 7.64 (ddd, J = 8.5, 7.4, 1.7 Hz, 1H, Ar), 8.02 (dd, J = 8.1, 1.7 Hz, 1H, Ar), 9.44 (br s, 1H, NH). MS (ES, positive mode): 353 $(M + Na)^+$, 661 $(2\ M + H)^+$.

*4.1.1.8. tert-Butyl (2-methoxy-4-(2-nitrophenoxy)phenyl)carbamate (**13h**).* Following the general procedure A, to a mixture of Cs_2CO_3 (227 mg, 0.70 mmol) and *tert*-butyl(4-hydroxy-2-methoxyphenyl) carbamate (**12h**) [22] (200 mg, 0.84 mmol) in CH_3CN (1.8 mL), 1-fluoro-2-nitrobenzene (**11**) (74 μL, 0.70 mmol) was added dropwise while stirring under argon. After 4 h at 80 °C, the residue was worked up and purified by flash chromatography (hexane/ethyl acetate, 4:1) to yield 212 mg (96%) of **13h** as a yellow oil. ^{1}H NMR (DMSO-d_6, 400 MHz): δ 1.45 (s, 9H, $(CH_3)_3$), 3.78 (s, 3H, OCH_3), 6.58 (dd, J = 8.7, 2.6 Hz, 1H, Ar), 6.87 (d, J = 2.6 Hz, 1H, Ar), 7.08 (dd, J = 8.4, 1.2 Hz, 1H, Ar), 7.31 (ddd, J = 8.4, 7.4, 1.2 Hz, 1H, Ar), 7.60–7.69 (m, 2H, Ar), 8.02 (br s, 1H, NH), 8.04 (dd, J = 8.2, 1.7 Hz, 1H, Ar). MS (ES, positive mode): 361 $(M + H)^+$, 383 $(M + Na)^+$, 721 $(2\ M + H)^+$.

*4.1.1.9. 1-(4-(2-Nitrophenoxy)acetophenone (**13i**).* Following the general procedure A, to a mixture of Cs_2CO_3 (925 mg, 2.84 mmol) and 4-hydroxyacetophenone (**12i**) (464 mg, 3.40 mmol) in CH_3CN (7.1 mL), 1-fluoro-2-nitrobenzene (**11**) (299 μL, 2.84 mmol) was added. After 5 h at 80 °C, the residue was worked up and purified by flash chromatography (dichloromethane/methanol, 20:1) to yield 613 mg (84%) of **13i** as a white solid. Mp 104–106 °C (lit [30] 104.6 °C). ^{1}H NMR (DMSO-d_6, 400 MHz): δ 2.56 (s, 3H, CH_3), 7.07–7.15 (m, 2H, Ar), 7.37 (dd, J = 8.3, 1.2 Hz, 1H, Ar), 7.50 (m, 1H, Ar), 7.79 (m, 1H, Ar), 7.98–8.03 (m, 2H, Ar), 8.14 (dd, J = 8.2, 1.6 Hz, 1H, Ar). MS (ES, positive mode): 258 $(M + H)^+$, 515 $(2\ M + H)^+$ ^{1}H NMR data are similar to those previously described [30].

4.1.2. General procedure for the synthesis of 2-aminodiphenyl ethers (general procedure B)

The corresponding 2-nitrodiphenyl ether was dissolved in ethyl acetate (12 mL) in a pressure vessel and then 10% Pd/C or 5% Pt/S (catalytic amount) was added. The vessel was hydrogenated at 30 psi for 1–5 h at room temperature. Then, the reaction mixture was filtered and volatiles were removed under reduced pressure. In most cases, the obtained 2-aminodiphenyl ethers were directly used as such in the subsequent reaction without further purification.

*4.1.2.1. 2-(3-Fluorophenoxy)aniline (**14a**).* Following the general procedure B, a solution of **13a** (431 mg, 1.85 mmol) in ethyl acetate (12 mL) in the presence of 5% Pt/S (catalytic amount) was subjected to hydrogenation for 2 h at rt. Then, the reaction mixture was filtered and the solvent was evaporated. The residue was purified by flash chromatography (hexane/ethyl acetate, 5:1) to afford 316 mg (84%) of **14a** as a colorless oil. **^{1}H NMR** (DMSO-d_6, 300 MHz): δ 4.95 (br s, 2H, NH_2), 6.52–6.60 (m, 1H, Ar), 6.62–6.72 (m, 2H, Ar), 6.78–6.90 (m, 3H, Ar), 6.95 (m, 1H, Ar), 7.27–7.39 (m, 1H, Ar). MS (ES, positive mode): 246 $(M + ACN + H)^+$. ^{1}H NMR data are similar to those previously described [28].

*4.1.2.2. 2-(4-Chlorophenoxy)aniline (**14b**).* Following the general procedure B, a solution of **13b** (63 mg, 0.252 mmol) in ethyl acetate (12 mL) in the presence of 5% Pt/S (catalytic amount) was subjected to hydrogenation for 2 h at rt. Then, the reaction mixture was filtered and the solvent was evaporated. The residue was purified by flash chromatography (hexane/ethyl acetate, 10:3) to afford 41 mg (74%) of **14b** as a colorless oil. ^{1}H NMR (DMSO-d_6, 300 MHz): δ 5.76 (br s, 2H, NH_2), 6.76–6.92 (m, 2H, Ar), 6.98–7.18 (m, 4H, Ar), 7.35–7.48 (m, 2H, Ar). MS (ES, positive mode): 220 $(M + H)^+$ with Cl isotopic distribution. ^{1}H NMR data are similar to those previously described [19].

*4.1.2.3. 2-(3-Methoxyphenoxy)aniline (**14c**).* Following the general procedure B, a solution of **13c** (400 mg, 1.63 mmol) in ethyl acetate (12 mL) in the presence of 10% Pd/C (catalytic amount) was subjected to hydrogenation for 2 h at rt. Then, the reaction mixture was filtered and the solvent was evaporated to afford 346 mg (98%) of **14c** as an orange oil. ^{1}H NMR (DMSO-d_6, 400 MHz): δ 3.71 (s, 3H, CH_3), 4.88 (br s, 2H, NH_2), 6.42 (ddd, J = 8.1, 2.3, 0.9 Hz, 1H, Ar), 6.47 (t, J = 2.4 Hz, 1H, Ar), 6.55 (ddd, J = 7.9, 7.2, 1.6 Hz, 1H, Ar), 6.62 (ddd, J = 8.3, 2.4, 0.9 Hz, 1H, Ar), 6.80 (dd, J = 7.9, 1.6 Hz, 2H, Ar), 6.92 (ddd, J = 8.0, 7.3, 1.5 Hz, 1H, Ar), 7.20 (t, J = 8.2 Hz, 1H, Ar). MS (ES, positive mode): 216 $(M + H)^+$, 257 $(M + ACN + H)^+$. ^{1}H NMR data are similar to those previously described [19].

*4.1.2.4. 2-(4-Methoxyphenoxy)aniline (**14d**).* Following the general procedure B, a solution of **13d** (648 mg, 2.64 mmol) in ethyl acetate (12 mL) in the presence of 10% Pd/C (catalytic amount) was subjected to hydrogenation for 2 h at rt. Then, the reaction mixture was filtered and the solvent was evaporated to afford 560 mg (98%) of **14d** as a pink oil. ^{1}H NMR (DMSO-d_6, 300 MHz): δ 3.71 (s, 1H, CH_3), 4.88 (br s, 2H, NH_2), 6.50 (m, 1H, Ar), 6.66 (dd, J = 8.0, 1.4 Hz, 1H, Ar), 6.76 (dd, J = 7.9, 1.7 Hz, 1H, Ar), 6.81–6.93 (m, 5H, Ar). MS (ES, positive mode): 216 $(M + H)^+$, 257 $(M + ACN + H)^+$. ^{1}H NMR data are similar to those previously described [31].

*4.1.2.5. 2-(3,4-Dimethoxyphenoxy)aniline (**14e**).* Following the general procedure B, a solution of **13e** (400 mg, 1.45 mmol) in ethyl acetate (12 mL) in the presence of 10% Pd/C (catalytic amount) was subjected to hydrogenation for 2 h at rt. Then, the reaction mixture was filtered and the solvent was evaporated to afford 343 mg (96%) of **14e** as a white solid. Mp 115–117 °C. ^{1}H NMR (DMSO-d_6, 400 MHz): δ 3.70 (s, 3H, OCH_3), 3.71 (s, 3H, OCH_3), 4.86 (br s, 2H, NH_2), 6.34 (m, 1H, Ar), 6.51 (m, 1H, Ar), 6.67–6.72 (m, 2H, Ar), 6.77 (m, 1H, Ar), 6.83–6.89 (m, 2H, Ar). MS (ES, positive mode): 246 $(M + H)^+$, 287 $(M + ACN + H)^+$. ^{1}H NMR data are similar to those previously described [32].

*4.1.2.6. tert-Butyl (3-(2-aminophenoxy)phenyl)carbamate (**14f**).* Following the general procedure B, a solution of **13f** (530 mg, 1.60 mmol) in ethyl acetate (12 mL) in the presence of 10% Pd/C (catalytic amount) was subjected to hydrogenation for 2 h at rt. Then, the reaction mixture was filtered and the solvent was evaporated to afford 490 mg (99%) of **14f** as a pink oil. ^{1}H NMR (DMSO-d_6, 400 MHz): δ 1.44 (s, 9H, $(CH_3)_3$), 4.85 (br s, 2H, NH_2), 6.47 (ddd, J = 8.1, 2.4, 1.1 Hz, 1H, Ar), 6.54 (ddd, J = 7.9, 7.2, 1.6 Hz, 1H, Ar), 6.75 (dd, J = 8.0, 1.4 Hz, 1H, Ar), 6.79 (dd, J = 7.9, 1.6 Hz, 1H, Ar), 6.90 (ddd, J = 7.9, 7.2, 1.5 Hz, 1H, Ar), 7.08–7.19 (m, 3H, Ar), 9.37 (br s, 1H, CONH). MS (ES, positive mode): 301 $(M + H)^+$, 601 $(2\ M + H)^+$.

*4.1.2.7. tert-Butyl (4-(2-aminophenoxy)phenyl)carbamate (**14g**).* Following the general procedure B, a solution of **13g** (275 mg, 0.83 mmol) in ethyl acetate (12 mL) in the presence of 10% Pd/C (catalytic amount) was subjected to hydrogenation for 1 h at rt. Then, the reaction mixture was filtered and the solvent was evaporated to afford 229 mg (92%) of **14f** as a pink oil. ^{1}H NMR (DMSO-d_6, 400 MHz): δ 1.46 (s, 9H, $(CH_3)_3$), 4.86 (br s, 2H, NH_2), 6.50 (m, 1H, Ar), 6.68 (dd, J = 8.1, 1.4 Hz, 1H, Ar), 6.77 (dd, J = 7.9, 1.7 Hz, 1H, Ar), 6.80–6.90 (m, 3H, Ar), 7.38 (d, J = 8.5 Hz, 2H), 9.24 (br s, 1H, NH). MS (ES, positive mode): 301 $(M + H)^+$, 601 $(2\ M + H)^+$.

*4.1.2.8. tert-Butyl (4-(2-aminophenoxy)-2-methoxyphenyl)carbamate (**14h**).* Following the general procedure B, a solution of **13h** (190 mg, 0.53 mmol) in ethyl acetate (12 mL) in the presence of 10% Pd/C (catalytic amount) was subjected to hydrogenation for 4 h at rt. Then, the reaction mixture was filtered and the solvent was evaporated to afford 150 mg (86%) of **14h** as a pink oil. ^{1}H NMR (DMSO-d_6, 400 MHz): δ 1.43 (s, 9H, $(CH_3)_3$), 3.75 (s, 3H, OCH_3), 4.87 (br s, 2H, NH_2), 6.33 (dd, J = 8.7, 2.6 Hz, 1H, Ar), 6.53 (m, 1H, Ar), 6.69 (d, J = 2.6 Hz, 1H, Ar), 6.75 (dd, J = 8.0, 1.4 Hz, 1H, Ar), 6.79 (dd, J = 7.9, 1.6 Hz, 1H, Ar), 6.89 (m, 1H, Ar), 7.43 (d, J = 8.7 Hz, 1H, Ar), 7.88 (br s, 1H, CONH). MS (ES, positive mode): 331 $(M + H)^+$, 661 $(2\ M + H)^+$.

*4.1.2.9. 1-(4-(2-Aminophenoxy)phenyl)ethan-1-one (**14i**) and 1-(4-(2-Aminophenoxy)phenyl)ethan-1-ol (**14j**).* Following the general procedure B, a solution of **13i** (250 mg, 0.97 mmol) in ethyl acetate (12 mL) in the presence of 10% Pd/C (catalytic amount) was subjected to hydrogenation for 1 h at rt. Then, the reaction mixture was filtered and the solvent was evaporated. The residue was purified by flash chromatography (hexane/ethyl acetate 2:1). The fastest moving fractions afforded 114 mg (52%) of **14i** as a colorless oil. ^{1}H NMR (DMSO-d_6, 300 MHz): δ 2.50 (s, 1H, CH_3), 4.96 (br s, 2H, NH_2), 6.58 (m, 1H, Ar), 6.79–7.01 (m, 5H, Ar), 7.92 (d, J = 8.4 Hz, 2H, Ar). MS (ES, positive mode): 228 $(M + H)^+$.

The slowest moving fractions afforded 93 mg (42%) of **14j** as a colorless oil. ^{1}H NMR (DMSO-d_6, 300 MHz): δ 1.29 (d, J = 6.4 Hz, 3H, CH_3), 4.67 (m, 1H, CH), 4.87 (br s, 1H, NH), 5.08 (d, J = 4.1 Hz, 1H, OH), 6.53 (m, 1H, Ar), 6.72–6.85 (m, 4H, Ar), 6.90 (m, 1H, Ar), 7.27 (d, J = 7.7 Hz, 2H, Ar). MS (ES, positive mode): 230 $(M + H)^+$.

4.1.3. General procedure for the reaction of 2-acetylcylcohexanedione with anilines (general procedure C)

A solution of 2-acetylcylcohexanedione (**15**) (1.0 mmol), the appropriate aniline (1.5 mmol) and 4 Å molecular sieves in toluene (10 mL) was placed in an Ace pressure tube [23]. Then, the vessel was sealed and heated in a microwave reactor at 110 °C overnight. After cooling, the solvent was evaporated and the residue was purified by flash chromatography or by CCTLC in the Chromatotron.

*4.1.3.1. 2-(1-((2-(3-Fluorophenoxy)phenyl)amino)ethylidene)-5-phenylcyclohexane-1,3-dione (**16a**).* Following the general procedure C, an Ace pressure tube was charged with **15** (189 mg, 0.82 mmol), **14a** (250 mg, 1.23 mmol) and 4 Å molecular sieves in toluene (5 mL). The resulting residue was purified by flash chromatography (hexane/ethyl acetate, 5:1) to afford 340 mg (99%) of **16a** as a brown oil. ^{1}H NMR (DMSO-d_6, 400 MHz): δ 2.44 (s, 3H,

CH_3), 2.50–2.61 (m, 2H, H-4, H-6), 2.68–2.88 (m, 2H, H-4, H-6), 3.27 (tt, $J = 12.0$, 4.1 Hz, 1H, H-5), 6.80 (dd, $J = 8.3$, 2.3 Hz, 1H, Ar), 6.90 (m, 1H, Ar), 7.00 (td, $J = 8.4$, 2.5 Hz, 1H, Ar), 7.16 (dd, $J = 8.2$, 1.3 Hz, 1H, Ar), 7.22 (m, 1H, Ar), 7.28–7.35 (m, 5H, Ar), 7.37–7.47 (m, 2H, Ar), 7.52 (dd, $J = 7.9$, 1.6 Hz, 1H, Ar), 14.84 (br s, 1H, NH). ^{13}C NMR (DMSO-d_6, 100 MHz): δ 19.8 (CH_3), 36.0 (C-5), 45.2 (C-4, C-6), 105.8 (d, $J = 24.8$ Hz, Ar), 108.6 (NHC=C), 110.6 (d, $J = 21.1$ Hz, Ar), 113.9 (d, $J = 3.0$ Hz, Ar), 120.3, 125.00, 126.5, 126.7, 127.7, 128.2, 128.5, 129.6 (Ar), 131.4 (d, $J = 9.9$ Hz, Ar), 143.4, 149.9, 157.5 (d, $J = 11.0$ Hz, Ar), 162.8 (d, $J = 245.0$ Hz, Ar), 172.5 (NHC=C). MS (ES, positive mode): 416 $(M + H)^+$. Anal. calc. for ($C_{26}H_{22}FNO_3$): C, 75.17; H, 5.34; N, 3.37. Found: C, 74.85; H, 5.46; N, 3.37.

*4.1.3.2. 2-(1-((2-(4-Chlorophenoxy)phenyl)amino)ethylidene)-5-phenylcyclohexane-1,3-dione (**16b**).* Following the general procedure C, an Ace pressure tube was charged with **15** (53 mg, 0.23 mmol), **14b** (34 mg, 0.15 mmol) and 4 Å molecular sieves in toluene (0.7 mL). The resulting residue was purified by CCTLC (hexane/ethyl acetate, 10:3) to afford 50 mg (75%) of **16b** as a brown oil. ^{1}H NMR (DMSO-d_6, 300 MHz): δ 2.45 (s, 3H, CH_3), 2.54–2.62 (m, 2H, H-4, H-6), 2.68–2.88 (m, 2H, H-4, H-6), 3.27 (m, 1H, H-5), 6.98–7.04 (m, 2H, Ar), 7.11 (dd, $J = 8.2$, 1.4 Hz, 1H, Ar), 7.22 (m, 1H, Ar), 7.28–7.34 (m, 5H, Ar), 7.39–7.46 (m, 3H, Ar), 7.51 (dd, $J = 7.8$, 1.7 Hz, 1H, Ar), 14.84 (br s, 1H, NH). ^{13}C NMR (DMSO-d_6, 100 MHz): δ 20.5 (CH_3), 36.7 (C-5), 45.6 (C-4, C-6), 109.3 (NHC=C), 120.6, 120.60, 125.0, 127.2, 127.4, 128.2, 128.3, 128.8, 129.2, 130.2, 130.6, 144.1, 150.9, 155.7 (Ar), 173.1 (NHC=C). MS (ES, positive mode): 432 $(M + H)^+$ with Cl isotopic distribution pattern. Anal. calc. for ($C_{26}H_{22}ClNO_3$): C, 72.30; H, 5.13; N, 3.24. Found: C, 71.95; H, 5.20; N, 3.38.

*4.1.3.3. 2-(1-((2-(3-Methoxyphenoxy)phenyl)amino)ethylidene)-5-phenylcyclohexane-1,3-dione (**16c**).* Following the general procedure C, an Ace pressure tube was charged with **15** (65 mg, 0.28 mmol), **14c** (92 mg, 0.42 mmol) and 4 Å molecular sieves in toluene (1.1 mL). The resulting residue was purified by CCTLC (hexane/ethyl acetate, 10:3) to afford 84 mg (70%) of **16c** as an oil. ^{1}H NMR (DMSO-d_6, 400 MHz): δ 2.45 (s, 3H, CH_3), 2.53–2.61 (m, 2H, H-4, H-6), 2.68–2.87 (m, 2H, H-4, H-6), 3.28 (tt, $J = 12.1$, 4.1 Hz, 1H, H-5), 3.73 (s, 1H, OCH_3), 6.51 (ddd, $J = 8.2$, 2.4, 0.8 Hz, 1H, Ar), 6.59 (t, $J = 2.4$ Hz, 1H, Ar), 6.74 (ddd, $J = 8.3$, 2.5, 0.8 Hz, 1H, Ar), 7.08 (dd, $J = 8.2$, 1.3 Hz, 1H, Ar), 7.18–7.24 (m, 1H, Ar), 7.25–7.37 (m, 6H, Ar), 7.41 (td, $J = 7.8$, 1.7 Hz, 1H, Ar), 7.49 (dd, $J = 7.8$, 1.6 Hz, 1H, Ar), 14.87 (br s, 1H, NH). ^{13}C NMR (DMSO-d_6, 125 MHz): δ 19.3 (CH_3), 36.0 (C-5), 45.1 (C-4, C-6), 55.3 (OCH_3), 104.5 (Ar), 108.6 (NHC=C), 109.8, 110.2, 119.6, 124.3, 126.5, 126.7, 127.4, 128.0, 128.5, 129.4, 130.6, 143.4, 150.7, 157.1, 160.7 (Ar), 172.5 (NHC=C). MS (ES, positive mode): 428 $(M + H)^+$. Anal. calc. for ($C_{27}H_{25}NO_4$): C, 75.86; H, 5.89; N, 3.28. Found: C, 75.55; H, 6.01; N, 3.29.

*4.1.3.4. 2-(1-((2-(4-Methoxyphenoxy)phenyl)amino)ethylidene)-5-phenylcyclohexane-1,3-dione (**16d**).* Following the general procedure C, an Ace pressure tube was charged with **15** (100 mg, 0.43 mmol), **14d** (139 mg, 0.65 mmol) and 4 Å molecular sieves in toluene (1.8 mL). The resulting residue was purified by flash chromatography (dichloromethane/methanol, 10:0.1) to afford 156 mg (85%) of **16d** as a white solid. Mp 137–139 °C. ^{1}H NMR (DMSO-d_6, 400 MHz): δ 2.48 (s, 3H, CH_3), 2.52–2.64 (m, 2H, H-4, H-6), 2.69–2.90 (m, 2H, H-4, H-6), 3.25 (m, 1H, H-5), 3.75 (s, 3H, OCH_3), 6.88 (dd, $J = 8.3$, 1.3 Hz, 1H, Ar), 6.94–7.03 (m, 4H, Ar), 7.16–7.27 (m, 2H, Ar), 7.29–7.38 (m, 5H, Ar), 7.45 (dd, $J = 7.9$, 1.6 Hz, 1H, Ar), 14.90 (br s, 1H, NH). ^{13}C NMR (DMSO-d_6, 100 MHz): δ 19.9 (CH_3), 36.0 (C-5), 45.6 (C-4, C-6), 55.5 (OCH_3), 108.6 (NHC=C), 115.2, 117.6, 120.6, 123.2, 126.3, 126.5, 126.7, 127.8, 128.5, 129.3, 143.5, 148.7, 152.0, 156.0 (Ar), 172.6 (NHC=C). MS (ES, positive mode): 428 $(M + H)^+$, 855 $(2\ M + H)^+$. Anal. calc. for ($C_{27}H_{25}NO_4$): C, 75.86; H, 5.89; N, 3.28. Found: C, 75.71; H, 5.98; N, 3.42.

*4.1.3.5. 2-(1-((2-(3,4-Dimethoxyphenoxy)phenyl)amino)ethylidene)-5-phenylcyclohexane-1,3-dione (**16e**).* Following the general procedure C, an Ace pressure tube was charged with **15** (48 mg, 0.21 mmol), **14e** (79 mg, 0.32 mmol) and 4 Å molecular sieves in toluene (0.8 mL). The resulting residue was purified by CCTLC (hexane/ethyl acetate, 2:1) to afford 73 mg (76%) of **16e** as a white solid. Mp 65–67 °C ^{1}H NMR (DMSO-d_6, 400 MHz): δ 2.48 (s, 3H, CH_3), 2.53–2.62 (m, 2H, H-4, H-6), 2.71–2.88 (m, 2H, H-4, H-6), 3.29 (m, 1H, H-5), 3.72 (s, 3H, OCH_3), 3.74 (s, 3H, OCH_3), 6.52 (dd, $J = 8.7$, 2.8 Hz, 1H, Ar), 6.76 (d, $J = 2.8$ Hz, 1H, Ar), 6.90–6.96 (m, 2H, Ar), 7.15–7.28 (m, 2H, Ar), 7.28–7.40 (m, 5H, Ar), 7.45 (dd, $J = 7.9$, 1.6 Hz, 1H, Ar), 14.89 (br s, 1H, NH). ^{13}C NMR (DMSO-d_6, 100 MHz): δ 20.0 (CH_3), 36.1 (C-5), 45.2 (C-4, C-6), 55.7 (OCH_3), 55.9 (OCH_3), 104.7 (Ar), 108.5 (NHC=C), 110.4, 112.5, 117.8, 123.2, 126.3, 126.5, 126.7, 127.8, 128.5, 129.3, 143.5, 145.7, 149.00, 149.8, 152.0 (Ar), 172.7 (NHC=C). MS (ES, positive mode): 458 $(M + H)^+$, 915 $(2\ M + H)^+$. Anal. calc. for ($C_{28}H_{27}NO_5$): C, 73.51; H, 5.95; N, 3.06. Found: C, 73.32; H, 6.00; N, 3.24.

*4.1.3.6. tert-Butyl (3-(2-((1-(2,6-dioxo-4-phenylcyclohexylidene) ethyl)amino)phenoxy)phenyl)carbamate (**16f**).* Following the general procedure C, an Ace pressure tube was charged with **15** (110 mg, 0.48 mmol), **14f** (215 mg, 0.72 mmol) and 4 Å molecular sieves in toluene (2 mL). The resulting residue was purified by CCTLC (hexane/ethyl acetate, 2:1) to afford 153 mg (71%) of **16f** as a white solid. Mp 159–161 °C. ^{1}H NMR (DMSO-d_6, 400 MHz): δ 1.43 (s, 9H, $(CH_3)_3$), 2.44 (s, 3H, CH_3), 2.52–2.64 (m, 2H, H-4, H-6), 2.68–2.84 (m, 2H, H-4, H-6), 3.27 (tt, $J = 12.2$, 4.0 Hz, 1H, H-5), 6.54 (m, 1H, Ar), 7.08 (dd, $J = 8.2$, 1.3 Hz, 1H, Ar), 7.15–7.25 (m, 4H, Ar), 7.28 (m, 1H, Ar), 7.28–7.37 (m, 4H, Ar), 7.41 (m, 1H, Ar), 7.49 (dd, $J = 7.8$, 1.6 Hz, 1H, Ar), 9.46 (br s, 1H, CONH), 14.85 (br s, 1H, NH). ^{13}C NMR (DMSO-d_6, 100 MHz): δ 19.8 (CH_3), 28.0 ($(CH_3)_3$), 36.0 (C-5), 46.3 (C-4, C-6), 79.3 ($C(CH_3)_3$), 108.5 (NHC=C), 107.7 111.5, 113.4, 119.8, 124.3, 126.5, 126.7, 127.5, 128.0, 128.5, 129.4, 130.0, 141.2, 143.5, 150.6, 152.6 (CONH), 156.4 (Ar), 172.5 (NHC=C). MS (ES, positive mode): 513 $(M + H)^+$. Anal. calc. for ($C_{31}H_{32}N_2O_5$): C, 72.64; H, 6.29; N, 5.47. Found: C, 72.52; H, 6.34; N, 5.74.

*4.1.3.7. tert-Butyl (4-(2-((1-(2,6-dioxo-4-phenylcyclohexylidene) ethyl)amino)phenoxy)phenyl)carbamate (**16g**).* Following the general procedure C, an Ace pressure tube was charged with **15** (100 mg, 0.43 mmol), **14g** (195 mg, 0.65 mmol) and 4 Å molecular sieves in toluene (1.9 mL). The resulting residue was purified by CCTLC (hexane/ethyl acetate, 2:1) to afford 192 mg (87%) of **16g** as a white solid. Mp 108–110 °C. ^{1}H NMR (DMSO-d_6, 400 MHz): δ 1.46 (s, 9H, $(CH_3)_3$), 2.46 (s, 3H, CH_3), 2.53–2.56 (m, 2H, H-4, H-6), 2.68–2.87 (m, 2H, H-4, H-6), 3.28 (m, 1H, H-5), 6.91–6.96 (m, 3H, Ar), 7.18–7.25 (m, 2H, Ar), 7.30–7.34 (m, 4H, Ar), 7.36 (ddd, $J = 8.3$, 7.5, 1.7 Hz, 1H, Ar), 7.44–7.48 (m, 3H, Ar), 9.38 (br s, 1H, CONH), 14.88 (br s, 1H, NH). ^{13}C NMR (DMSO-d_6, 100 MHz): δ 19.9 (CH_3), 28.1 ($(CH_3)_3$), 36.0 (C-5), 45.9 (C-4, C-6), 79.0 ($C(CH_3)_3$), 108.6 (NHC=C), 118.2, 119.4, 119.7, 123.4, 126.5, 126.6, 126.7, 127.9, 128.5, 129.3, 136.0, 143.5, 150.0, 151.6 (Ar), 152.8 (CONH), 172.5 (NHC=C). MS (ES, positive mode): 513 $(M + H)^+$. Anal. calc. for ($C_{31}H_{32}N_2O_5$): C, 72.64; H, 6.29; N, 5.47. Found: C, 72.29; H, 6.39; N, 5.65.

*4.1.3.8. tert-Butyl (4-(2-((1-(2,6-dioxo-4-phenylcyclohexylidene) ethyl)amino)phenoxy)methoxyphenyl)carbamate (**16h**).* Following the general procedure C, an Ace pressure tube was charged with **15** (65 mg, 0.28 mmol), **14h** (62 mg, 0.19 mmol) and 4 Å molecular sieves in toluene (0.8 mL). The resulting residue was purified by CCTLC (hexane/ethyl acetate, 3:1) to afford 78 mg (76%)

of **16h** as a white solid. Mp 189–191 °C. ^{1}H NMR (DMSO-d_6, 400 MHz): δ 1.44 (s, 9H, $(CH_3)_3$), 2.47 (s, 3H, CH_3), 2.53–2.66 (m, 2H, H-4, H-6), 2.69–2.91 (m, 2H, H-4, H-6), 3.28 (m, 1H, H-5), 3.76 (s, 3H, OCH_3), 6.49 (dd, J = 8.7, 2.6 Hz, 1H, Ar), 6.76 (d, J = 2.6 Hz, 1H, Ar), 7.00 (dd, J = 8.2, 1.3 Hz, 1H, Ar), 7.20–7.26 (m, 2H, Ar), 7.32 (m, 4H, Ar), 7.38 (m, 1H, Ar), 7.47 (dd, J = 7.9, 1.6 Hz, 1H, Ar), 7.57 (d, J = 8.7 Hz, 1H, Ar), 7.99 (br s, 1H, CONH), 14.89 (br s, 1H, NH). ^{13}C NMR (DMSO-d_6, 100 MHz): δ 19.9 (CH_3), 28.1 ((CH_3)$_3$), 36.1 (C-5), 45.5 (C-4, C-6), 55.9 (OCH_3), 79.1 (C(CH_3)$_3$), 103.3 (Ar), 108.6 (NHC=C), 109.9, 118.6, 122.6, 123.7, 126.5, 126.8, 128.0, 128.5, 129.4, 143.5, 151.3 (Ar), 151.9 (CONH), 153.0 (Ar), 172.6 (NHC=C). MS (ES, positive mode): 543 $(M + H)^+$. Anal. calc. for ($C_{32}H_{34}N_2O_6$): C, 70.83; H, 6.32; N, 5.16. Found: C, 70.60; H, 6.33; N, 5.37.

*4.1.3.9. 2-(1-((2-(4-Acetylphenoxy)phenyl)amino)ethylidene)-5-phenylcyclohexane-1,3-dione (**16i**).* Following the general procedure C, an Ace pressure tube was charged with **15** (26 mg, 0.11 mmol), 1**4i** (39 mg, 0.17 mmol) and 4 Å molecular sieves in toluene (0.5 mL). The resulting residue was purified by CCTLC (hexane/ethyl acetate, 1:1) to afford 24 mg (48%) of **16i** as a white solid. Mp 103–105 °C. ^{1}H NMR (DMSO-d_6, 400 MHz): δ 2.45 (s, 3H, CH_3), 2.54 (s, 3H, $COCH_3$), 2.52–2.58 (m, 2H, H-4, H-6), 2.67–2.81 (m, 2H, H-4, H-6), 3.23 (tt, J = 12.0, 4.0 Hz, 1H, H-5), 7.01–7.06 (m, 2H, Ar), 7.20–7.34 (m, 6H, Ar), 7.37 (td, J = 7.7, 1.4 Hz, 1H, Ar), 7.48 (td, J = 7.8, 1.7 Hz, 1H, Ar), 7.55 (dd, J = 7.9, 1.7 Hz, 1H, Ar), 7.95–7.99 (m, 2H, Ar), 14.85 (br s, 1H, NH). ^{13}C NMR (DMSO-d_6, 100 MHz): δ 19.8 (CH_3), 26.6 ($COCH_3$), 36.0 (C-5), 45.0 (C-4, C-6), 108.6 (NHC=C), 117.1, 121.2, 125.6, 126.5, 126.7, 128.3, 128.3, 128.5, 129.7, 130.8, 132.3, 143.4, 149.2, 160.4, 172.4 (NHC=C), 196.5 ($COCH_3$). MS (ES, positive mode): 440 $(M + H)^+$. Anal. calc. for ($C_{28}H_{25}NO_4$): C, 76.52; H, 5.73; N, 3.19. Found: C, 76.12; H, 5.87; N, 3.24.

*4.1.3.10. 2-(1-((2-(4-(1-Hydroxyethyl)phenoxy)phenyl)amino)ethylidene)-5-phenylcyclohexane-1,3-dione (**16j**).* Following the general procedure C, an Ace pressure tube was charged with **15** (30 mg, 0.14 mmol), **14j** (46 mg, 0.20 mmol) and 4 Å molecular sieves in toluene (1 mL). The resulting residue was purified by CCTLC (hexane/ethyl acetate, 1; 1) to afford 16 mg (28%) of **16j** as a white solid. Mp 60–62 °C. ^{1}H NMR (DMSO-d_6, 500 MHz): δ 1.31 (d, J = 6.4 Hz, 3H, (CH_3)CHOH), 2.46 (s, 3H, CH_3), 2.54–2.61 (m, 2H, H-4, H-6), 2.70–2.84 (m, 2H, H-4, H-6), 3.28 (m, 1H, H-5), 4.71 (qd, J = 6.3, 4.1 Hz, 1H, CHOH), 5.16 (d, J = 4.2 Hz, 1H, OH), 6.93–6.97 (m, 2H, Ar), 7.00 (dd, J = 8.2, 1.3 Hz, 1H, Ar), 7.20–7.27 (m, 2H, Ar), 7.28–7.33 (m, 4H, Ar), 7.34–7.37 (m, 2H, Ar), 7.39 (td, J = 7.8, 1.7 Hz, 1H, Ar),7.48 (dd, J = 7.9, 1.6 Hz, 1H, Ar), 14.90 (br s, 1H, NH). ^{13}C NMR (DMSO-d_6, 125 MHz): δ 19.9 (CH_3), 26.0 ((CH_3CHOH), 36.0 (C-5), 45.3 (C-4, C-6), 67.5 (CHOH), 108.6 (NHC=C), 118.2, 119.0, 123.9, 126.5, 126.3, 127.0, 127.1, 127.9, 128.5, 129.4, 143.2, 143.5, 151.1, 154.4 (Ar), 172.5 (NHC=C). MS (ES, positive mode): 442 $(M + H)^+$. Analytical HPLC (gradient 15–95% acetonitrile in 10 min): T_R: 6.08; area: 100%. (gradient 50–70% acetonitrile in 10 min): T_R: 4.57; area: 100%.

*4.1.3.11. 2-(1-((2-Phenoxyphenyl)amino)ethylidene)-5-phenylcyclohexane-1,3-dione (**16k**).* Following the general procedure C, an Ace pressure tube was charged with **15** (58 mg, 0.26 mmol), 2-phenoxyaniline (**14k**) (73 mg, 0.39 mmol) and 4 Å molecular sieves in toluene (1.1 mL). The resulting residue was purified by CCTLC (hexane/ethyl acetate, 2:1) to afford 70 mg (68%) of **16k** as an oil. ^{1}H NMR (DMSO-d_6, 400 MHz): δ 2.46 (s, 3H, CH_3), 2.53–2.62 (m, 2H, H-4, H-6), 2.66–2.87 (m, 2H, H-4, H-6), 3.28 (m, 1H, H-5), 6.98–7.05 (m, 3H, Ar), 7.14–7.25 (m, 2H, Ar), 7.28 (dd, J = 7.6, 1.4 Hz, 1H, Ar), 7.30–7.38 (m, 5H, Ar), 7.40–7.44 (m, 2H, Ar), 7.49 (dd, J = 7.9, 1.7 Hz, 1H, Ar), 14.89 (br s, 1H, NH). ^{13}C NMR (DMSO-d_6, 100 MHz): δ 19.8 (CH_3), 36.0 (C-5), 45.8 (C-4, C-6), 108.6 (HNC=C), 118.4, 119.3, 124.0, 124.1, 126.5, 126.7, 127.3, 128.0, 128.5, 129.4, 130.2, 143.4, 150.8, 156.0 (Ar), 172.5 (HNC=C). MS (ES, positive mode): 398 $(M + H)^+$.Anal. calc. for ($C_{26}H_{30}N_2O_4$): C, 78.59; H, 5.83; N, 3.52. Found: C, 78.30; H, 5.95; N, 3.58.

*4.1.3.12. 2-(1-((2-(3-Aminophenoxy)phenyl)amino)ethylidene)-5-phenylcyclohexane-1,3-dione (**16l**).* To a solution of **16f** (60 mg, 0.12 mmol) in dichloromethane (0.4 mL), TFA (0.4 mL, 4.68 mmol) was added and the reaction mixture was stirred at room temperature for 30 min. Then volatiles were removed and the residue was purified by CCTLC (hexane/ethyl acetate, 1:1) to afford 47 mg (97%) of **16l** as a white solid. Mp 76–78 °C. ^{1}H NMR (DMSO-d_6, 400 MHz): δ 2.46 (s, 3H, CH_3), 2.53–2.63 (m, 2H, H-4, H-6), 2.68–2.88 (m, 2H, H-4, H-6), 3.30 (m, 1H, H-5), 5.27 (br s, 2H, NH_2), 6.08 (ddd, J = 8.0, 2.4, 0.9 Hz, 1H, Ar), 6.16 (t, J = 2.2 Hz, 1H, Ar), 6.34 (ddd, J = 8.1, 2.2, 0.9 Hz, 1H, Ar), 6.98 (t, J = 8.0 Hz, 1H, Ar), 7.04 (dd, J = 8.3, 1.3 Hz, 1H, Ar), 7.17–7.25 (m, 2H, Ar), 7.30–7.33 (m, 4H, Ar), 7.38 (td, J = 7.8, 1.6 Hz, 1H, Ar), 7.45 (dd, J = 7.9, 1.6 Hz, 1H, Ar), 14.87 (br s, 1H, NH). ^{13}C NMR (DMSO-d_6, 100 MHz): δ 19.8 (CH_3), 36.0 (C-5), 45.3 (C-4, C-6), 103.4, 105.4 (Ar), 108.5 (NHC=C), 109.7, 119.4, 123.7, 126.5, 126.7, 127.2, 127.8, 128.5, 129.3, 130.1, 143.5, 150.6, 151.0, 156.9 (Ar), 172.5 (NHC=C). MS (ES, positive mode): 413 $(M + H)^+$. Anal. calc. for ($C_{26}H_{24}N_2O_3 \cdot H_2O$): C, 72.54; H, 6.09; N, 6.51. Found: C, 72.86; H, 5.84; N, 6.89.

*4.1.3.13. 4-(2-((1-(2,6-Dioxo-4-phenylcyclohexylidene)ethyl)amino)phenoxy)benzen-aminium 2,2,2-trifluoroacetate (**16m**).* To a solution of **16g** (66 mg, 0.13 mmol) in dichloromethane (0.4 mL), TFA (0.4 mL, 5.07 mmol) was added and the reaction mixture was stirred at room temperature for 20 min. Then volatiles were removed and the residue was triturated with dichloromethane and hexane yielding 65 mg (99%) of **16m** as a white solid. Mp 73–75 °C. ^{1}H NMR (DMSO-d_6, 400 MHz): δ 2.46 (s, 3H, CH_3), 2.54–2.61 (m, 2H, H-4, H-6), 2.69–2.86 (m, 2H, H-4, H-6), 3.29 (tt, J = 12.1, 4.0 Hz, 1H, H-5), 7.00–7.07 (m, 3H, Ar), 7.15–7.20 (m, 2H, Ar), 7.20–7.36 (m, 6H, Ar), 7.41 (ddd, J = 8.3, 7.3, 1.7 Hz, 1H, Ar), 7.50 (dd, J = 7.9, 1.6 Hz, 1H, Ar), 14.89 (br s, 1H, NH). ^{13}C NMR (DMSO-d_6, 100 MHz): δ 19.9 (CH_3), 36.0 (C-5), 45.9 (C-4, C-6), 108.6 (NHC=C), 119.1, 119.6, 122.3, 124.2, 126.6, 126.7, 127.2, 128.0, 128.5, 129.5, 132.2, 143.4, 150.8, 152.8 (Ar), 158.2 (q, J = 34.2 Hz, CF_3COO^-), 172.6 (NHC=C). MS (ES, positive mode): 413 $(M + H)^+$ for $C_{26}H_{24}N_2O_3$. Anal. calc. for ($C_{28}H_{25}F_3N_2O_5 \cdot H_2O$): C, 63.87; H, 4.79; N, 5.32. Found: C, 63.50; H, 4.74; N, 5.14.

*4.1.3.14. 4-(2-((1-(2,6-Dioxo-4-phenylcyclohexylidene)ethyl)amino)phenoxy)-2-methoxybenzenaminium 2,2,2-trifluoroacetate (**16n**).* To a solution of **16h** (20 mg, 0.04 mmol) in dichloromethane (0.5 mL), TFA (0.1 mL, 1.47 mmol) was added and the reaction mixture was stirred at room temperature for 1 h. Then volatiles were removed and the residue was triturated with dichloromethane and hexane yielding 18 mg (88%) of **16n** as a white solid. Mp 79–81 °C. ^{1}H NMR (DMSO-d_6, 400 MHz): δ 2.48 (s, 3H, CH_3), 2.55–2.63 (m, 2H, H-4, H-6), 2.71–2.85 (m, 2H, H-4, H-6), 3.30 (tt, J = 12.1, 4.0 Hz, 1H, H-5), 3.82 (s, 3H, OCH_3), 6.50 (dd, J = 8.5, 2.5 Hz, 1H, Ar), 6.83 (d, J = 2.5 Hz, 1H, Ar), 7.00 (dd, J = 8.3, 1.3 Hz, 1H, Ar), 7.04 (d, J = 8.5 Hz, 1H, Ar), 7.20–7.26 (m, 2H, Ar), 7.30–7.34 (m, 4H, Ar), 7.39 (ddd, J = 8.2, 7.4, 1.7 Hz, 1H, Ar), 7.48 (dd, J = 7.9, 1.6 Hz, 1H, Ar), 14.88 (br s, 1H, NH). ^{13}C NMR (DMSO-d_6, 100 MHz): δ 19.9 (CH_3), 36.1 (C-5), 45.4 (C-4, C-6), 56.1 (OCH_3), 108.6 (NHC=C), 103.8, 110.6, 118.5, 120.3, 123.8, 126.6, 126.8, 128.0, 128.5, 129.4, 143.4, 150.9, 151.3 (Ar), 172.6 (NHC=C). MS (ES, positive mode): 443 $(M + H)^+$ for $C_{27}H_{26}N_2O_4$. Anal. calc. for ($C_{29}H_{27}F_3N_2O_6$): C, 62.59; H, 4.89; N, 5.03. Found: C, 62.22; H, 5.10; N, 5.21.

4.2. Biological methods

The human microvascular endothelial cell line HMEC-1 was obtained from the Centers for Disease Control and Prevention (Atlanta, GA, USA) and used from passage 17 till 27. Human cervical carcinoma (HeLa) and human T-lymphoid (CEM) cells were obtained from ATCC (Middlesex, UK). Cell lines were maintained in culture for up to 3 months and grown in DMEM, supplemented with 10% FBS, 0.01 M Hepes and 1 mM sodium pyruvate. All cells were cultured in a humidified 5% CO_2 incubator at 37 °C.

4.2.1. Cell proliferation

HMEC-1 cells were seeded in 48-well plates at 20,000 cells/well. After 24 h, 5-fold dilutions of the compounds were added. The cells were allowed to proliferate 4 days in the presence of the compounds, trypsinized, and counted by means of a Coulter counter (Analis, Belgium). Human cervical carcinoma (HeLa) cells were seeded in 48-well plates at 10,000 cells/well. After 24 h, different concentrations of the compounds were added. After 3 days of incubation, the cells were trypsinized and counted in a Coulter counter. Suspension cells (Mouse leukemia L1210 and human lymphoid CEM cells) were seeded in 96-well plates at 60,000 cells/well in the presence of different concentrations of the compounds, allowed to proliferate for 96 h, and counted in a Coulter counter. The 50% inhibitory concentration (IC_{50}) was defined as the compound concentration required to reduce cell proliferation by 50%.

4.2.2. Cell cycle analysis

HMEC-1 cells were seeded in 6-well plates at 125,000 cells/well in DMEM with 10% FBS. After 24 h, the cells were exposed to different concentrations of the compounds. After 24 h, the DNA of the cells was stained with propidium iodide using the CycleTEST PLUS DNA Reagent Kit (BD Biosciences, San Jose, CA). The DNA content of the stained cells was assessed by flow cytometry on a FACSCalibur flow cytometer and analyzed with CellQuest software (BD Biosciences) within 3 h after staining. Cell debris and clumps were excluded from the analysis by appropriate dot plot gating. Percentages of sub-G1, G1, S, and G_2/M cells were estimated using appropriate region markers [33].

4.2.3. Tube formation

Wells of a 96-well plate were coated with 70 μL matrigel (10 mg/mL, BD Biosciences, Heidelberg, Germany) at 4 °C. After gelatinization at 37 °C during 30 min, HMEC-1 cells were seeded at 60,000 cells/well on top of the matrigel in 200 μL DMEM containing 10% FCS. After 3 h of incubation at 37 °C, when the endothelial cells had reorganized to form tube-like structures, the compounds were added. Ninety minutes later, the cultures were photographed at 100× magnification and analyzed using digitalized analysis.

4.2.4. Determination of binding constants

Proteins and ligands. Calf brain tubulin was purified as described [34]. (*R*)-(+)-ethyl 5-amino 2-methyl-1,2-dihydro-3-phenylpyrido [3,4-*b*]pyrazin-7-yl carbamate (R-PT) [35] was a kind gift of Prof. G.A. Rener, Organic Chemistry Research Department, Southern Research Institute, Birminghm, Alabama. The compounds were diluted in 99.8% D6-DMSO (Merck, Darmstadt, Germany) to a final concentration of 20 mM and stored at −80 °C.

Determination of binding constants. The binding constant of R-PT [25] for dimeric tubulin was determined using the competition method in 10 mM sodium phosphate, 0.1 mM GTP pH 7.0 at 25 °C. To do so 0.2 μM of R-PT was incubated with increasing amounts of tubulin up to 10 μM and vice versa, 0.2 μM of tubulin was incubated with increasing amounts of R-PT up to 10 μM, the fluorescence emission spectra (excitation 374 nm) of the samples (5 nm excitation and emission slits) were determined using a Jobin-Ybon SPEX Fluoromax-2 (HORIBA, Ltd. Kyoto, Japan). Using these spectra it is possible to calculate the free and the bound R-PT concentration for each sample and thus to determine the binding constant of R-PT for tubulin.

Once K_b of R-PT is determined ($5.1 \times 10^6\ M^{-1}$) this compound could be used as a reference ligand as described in Ref. [36]. For that purpose, the fluorescence emission of a previous mixed sample of 0.2 μM of R-PT and 0.2 μM of tubulin was evaluated in the presence of increasing concentrations of the studied ligand in a black 96-well plate (0; 0.05; 0.2; 0.5; 2; 5; 10; 30; 50; 70 μM). The samples were incubated 30 min at 25 °C in a *Varioskan* plate reader (Thermo Scientific Waltham, Massachusetts, USA) before the fluorescence emission intensity at 456 nm (excitation 374 nm) was measured. The data were analyzed and the binding constants determined using Equigra V5.0 [37].

4.2.5. Tubulin assembly time-course

Tubulin was diluted at a final concentration of 25 μM in a 10 mM NaPi, 1 mM EGTA, 1 mM GTP (pH = 7) buffer supplemented with 3.4 M glycerol. Each polymerization reaction was prepared in a 96-well plate to a final volume of 100 μL with 30 μM of each of the compounds tested (or the equivalent volume of DMSO for the control). Polymerization was followed throughout time measuring the scattering of light (λ = 350 nm) using a Varioskan plate reader (Thermo Scientific Waltham, Massachusetts, USA).

4.3. Computational methods

4.3.1. Affinity maps calculation

Binding pocket analysis of the tubulin-DAMA-colchicine was carried out with cGRILL [17,18], a computational tools formally equivalent to Goodford's program GRID [38]. Hydrogen atoms, atom point charges and radii for all atoms in the complexes were calculated by submission to H++ server (http://biophysics.cs.vt.edu) in order to obtain their pqr format files. Grid center was defined by selecting the corresponding ligand and a cubic box of 50 × 50 × 50 points and a 0.5 Å was set for the calculations. cGRILL evaluates, at each grid point, the interaction energy between the whole receptor and five different probes combining van der Waals (Leonard-jones potential), electrostatic (Coulombic), and hydrogen bonding [39] (geometry based) terms.

The five calculated affinity maps: lipophilic (CH3), hydrogen bond acceptor (=O), hydrogen bond donor ($NH4^+$), mixed hydrogen bond donor-acceptor (OH) and hydrophobic-like (hydrophobic) were visualized and analyzed using the PyMOL plugin provided with the software.

4.3.2. Docking of ***16n***

Compound **16n** was used as ligand for the automated docking experiments using TUB075 tubulin complex (PDB ID: 6KFJ) [16]. AMBER-compatible RESP point charges were used for **16n**. The Lamarckian genetic algorithm implemented in AutoDock 4.2 [40] was used to generate the docked conformations within the putative binding cavity by randomly changing the overall orientation of the molecule as well as the torsion angles of all rotatable bonds. Default settings were used except for the number of runs, population size, and maximum number of energy evaluations, which were fixed at 250, 100 and 250.000, respectively. Rapid intra- and intermolecular energy evaluations of each configuration was achieved by having the receptor's atomic affinity potentials for aliphatic and aromatic carbon, oxygen, nitrogen and hydrogen atoms precalculated in a three-dimensional grid with a spacing of 0.375 Å. A distance-dependent dielectric function was used in the computation of electrostatic interactions.

Conflicts of interest

The authors declare that they have no competing interests.

Author contributions

M-J.P.P. and E-M.P. designed the ligands. O.B. and M.G. performed the chemical synthesis supervised by M-J.P.P. and M-J.C. J.E.-G. performed the binding affinity assays supervised by J.F.D. S.M. performed the biological assays supervised by S.L. M-J.P.P., S.L. and E-M.P wrote the manuscript.

Acknowledgments

This project has been supported by the Spanish Ministerio de Economía y Competitividad SAF2015-64629-C2-1-R (to EMP, MJPP. and MJC) and BFU2016-75319-R (AEI/FEDER, UE) (JFD.) Financial support from CSIC (Proyecto Intramural PIE-201668E079 to MJPP) is also acknowledged. The authors acknowledge networking contribution by COST action CM1407 "Challenging synthesis inspired by nature – from natural products chemistry to drug discovery" (to MJPP, SL, and JFD). JFD. is a member of the CIB Intramural Program "Molecular Machines for Better Life" (MAC-BET). We acknowledge Lizette Van Berckelaer, Eef Meyen and Sam Noppen for excellent technical assistance. We thank ganadería Fernando Díaz for calf brains for tubulin purification.

Appendix A. Supplementary data

Supplementary data to this article can be found online at https://doi.org/10.1016/j.ejmech.2019.03.045.

References

[1] G.J. Brouhard, L.M. Rice, Microtubule dynamics: an interplay of biochemistry and mechanics, Nat. Rev. Mol. Cell Biol. 19 (2018) 451–463. https://doi.org/10.1038/s41580-018-0009-y.
[2] C. Dumontet, M.A. Jordan, Microtubule-binding agents: a dynamic field of cancer therapeutics, Nat. Rev. Drug Discov. 9 (2010) 790–803. https://doi.org/10.1038/nrd3253.
[3] R. Kaur, G. Kaur, R.K. Gill, R. Soni, J. Bariwal, Recent developments in tubulin polymerization inhibitors: an overview, Eur. J. Med. Chem. 87 (2014) 89–124. https://doi.org/10.1016/j.ejmech.2014.09.051.
[4] R.A. Stanton, K.M. Gernert, J.H. Nettles, R. Aneja, Drugs that target dynamic microtubules: a new molecular perspective, Med. Res. Rev. 31 (2011) 443–481. https://doi.org/10.1002/med20242.
[5] Y. Zhao, X. Mu, G. Du, Microtubule-stabilizing agents: new drug discovery and cancer therapy, Pharmacol. Therapeut. 162 (2016) 134–143. https://doi.org/10.1016/j.pharmthera.2015.12.006.
[6] M.O. Steinmetz, A.E. Prota, Microtubule-targeting agents: strategies to hijack the cytoskeleton, Trends Cell Biol. 28 (2018) 776–792. https://doi.org/10.1016/j.tcb.2018.05.001.
[7] D. Bates, A. Eastman, Microtubule destabilising agents: far more than just antimitotic anticancer drugs, Br. J. Clin. Pharmacol. 83 (2017) 255–268. https://doi.org/10.1111/bcp.13126.
[8] L.M. Greene, M.J. Meegan, D.M. Zisterer, Combretastatins: more than just vascular targeting agents? J. Pharmacol. Exp. Ther. 355 (2015) 212–227. https://doi.org/10.1124/jpet.115.226225.
[9] P. Mabeta, M.S. Pepper, A comparative study on the anti-angiogenic effects of DNA-damaging and cytoskeletal-disrupting agents, Angiogenesis 12 (2009) 81–90. https://doi.org/10.1007/s10456-009-9134-8.
[10] D.W. Siemann, M.R. Horsman, Modulation of the tumor vasculature and oxygenation to improve therapy, Pharmacol. Ther. 153 (2015) 107–124. https://doi.org/10.1016/j.pharmthera.2015.06.006.
[11] C. Kanthou, G.M. Tozer, Microtubule depolymerizing vascular disrupting agents: novel therapeutic agents for oncology and other pathologies, Int. J. Exp. Pathol. 90 (2009) 284–294. https://doi.org/10.1111/j.1365-2613.2009.00651.x.
[12] M.J. Pérez-Pérez, E.M. Priego, O. Bueno, M.S. Martins, M.D. Canela, S. Liekens, Blocking blood flow to solid tumors by destabilizing tubulin: an approach to targeting tumor growth, J. Med. Chem. 59 (2016) 8685–8711. https://doi.org/10.1021/acs.jmedchem.6b00463.
[13] Y.T. Ji, Y.N. Liu, Z.P. Liu, Tubulin colchicine binding site inhibitors as vascular disrupting agents in clinical developments, Curr. Med. Chem. 22 (2015) 1348–1360. https://doi.org/10.2174/0929867322666150114163732.
[14] R.B.G. Ravelli, B. Gigant, P.A. Curmi, I. Jourdain, S. Lachkar, A. Sobel, M. Knossow, Insight into tubulin regulation from a complex with colchicine and a stathmin-like domain, Nature 428 (2004) 198–202. https://doi.org/10.1038/nature02393.
[15] A. Massarotti, A. Coluccia, R. Silvestri, G. Sorba, A. Brancale, The tubulin colchicine domain: a molecular modeling perspective, ChemMedChem 7 (2012) 33–42. https://doi.org/10.1002/cmdc.201100361.
[16] O. Bueno, J. Estévez Gallego, S. Martins, A.E. Prota, F. Gago, A. Gómez-SanJuan, M.-J. Camarasa, I. Barasoain, M.O. Steinmetz, J.F. Díaz, M.-J. Pérez-Pérez, S. Liekens, E.-M. Priego, High-affinity ligands of the colchicine domain in tubulin based on a structure-guided design, Sci. Rep. 8 (2018) 4242. https://doi.org/10.1038/s41598-018-22382-x.
[17] A. Cortés-Cabrera, F. Gago, A. Morreale, A computational fragment-based de novo design protocol guided by ligand efficiency indices (LEI), Methods in molecular biology (Clifton, N. J.) 1289 (2015) 89–100.
[18] F. Gago, Avaliable at, http://farmamol.uah.es.
[19] J. Hwang, P. Li, W.R. Carroll, M.D. Smith, P.J. Pellechia, K.D. Shimizu, Additivity of substituent effects in aromatic stacking interactions, J. Am. Chem. Soc. 136 (2014) 14060–14067. https://doi.org/10.1021/ja504378p.
[20] T. Tomasic, N. Zidar, R. Sink, A. Kovac, D. Blanot, C. Contreras-Martel, A. Dessen, M. Muller-Premru, A. Zega, S. Gobec, D. Kikelj, L. Peterlin Masic, Structure-based design of a new series of D-glutamic acid based inhibitors of bacterial UDP-N-acetylmuramoyl-L-alanine:D-glutamate Ligase (MurD), J. Med. Chem. 54 (2011) 4600–4610. https://doi.org/10.1021/jm2002525.
[21] A. Vigroux, M. Bergon, C. Zedde, Cyclization-Activated Prodrugs: N-(Substituted 2-hydroxyphenyl and 2-hydroxypropyl)carbamates based on ring-opened derivatives of active benzoxazolones and oxazolidinones as mutual prodrugs of acetaminophen, J. Med. Chem. 38 (1995) 3983–3994. https://doi.org/10.1021/jm00020a012.
[22] K.S. Lim, H. Lee, S.E. Kim, T.H. Ha, J. Ann, K. Son, S. Choi, W. Sun, L.V. Pearce, I.A. De Andrea-Lazarus, P.M. Blumberg, J. Lee, The carbonate analogues of 5'-halogenated resiniferatoxin as TRPV1 ligands, Eur. J. Med. Chem. 68 (2013) 233–243. https://doi.org/10.1016/j.ejmech.2013.07.042.
[23] M.D. Canela, M.J. Pérez-Pérez, S. Noppen, G. Saez-Calvo, J.F. Diaz, M.J. Camarasa, S. Liekens, E.M. Priego, Novel colchicine-site binders with a cyclohexanedione scaffold identified through a ligand-based virtual screening approach, J. Med. Chem. 57 (2014) 3924–3938. https://doi.org/10.1021/jm401939g.
[24] M.D. Canela, O. Bueno, S. Noppen, G. Saez Calvo, J. Estevez Gallego, J.F. Diaz, M.J. Camarasa, S. Liekens, M.J. Pérez-Pérez, E.M. Priego, Targeting the colchicine site in tubulin through cyclohexanedione derivatives, RSC Adv. 6 (2016) 19492–19506. https://doi.org/10.1039/C5RA26807A.
[25] D. Leynadie, V. Peyrot, M. Sarrazin, C. Briand, J.M. Andreu, G.A. Rener, C. Temple, Tubulin binding of two 1-deaza-7,8-dihydropteridines with different biological properties: enantiomers NSC 613862 (S)-(-) and NSC 613863 (R)-(+), Biochemistry 32 (1993) 10675–10682. https://doi.org/10.1021/bi00091a018.
[26] J.F. Diaz, J.M. Andreu, Kinetics of dissociation of the tubulin-colchicine complex - complete reaction scheme and comparison to thermodynamic measurements, J. Biol. Chem. 266 (1991) 2890–2896.
[27] F. Cortese, B. Bhattacharyya, J. Wolff, Podophyllotoxin as a probe for colchicine binding-site of tubulin, J. Biol. Chem. 252 (1977) 1134–1140.
[28] L.F. Tietze, T. Hungerland, A. Duefert, I. Objartel, D. Stalke, Synthesis of tetrasubstituted alkenes through a palladium-catalyzed domino carbopalladation/C-H-activation reaction, Chem. Eur J. 18 (2012) 3286–3291. https://doi.org/10.1002/chem.201103209.
[29] J.D.C. Mole, E.E. Turner, Intramolecular substitution as a means of comparing activating and deactivating effects, J. Chem. Soc. (1939) 1720–1724. https://doi.org/10.1039/jr9390001720.
[30] M. Huang, L. Wang, X. Li, S. Yan, K.W.K. Yeung, P.K. Chu, Z. Xu, C. Yi, Design and preparation of novel fluorescent polyimides containing ortho-linked units and pyridine moieties, Des. Monomers Polym 15 (2012) 389–404. https://doi.org/10.1080/1385772X.2012.686691.
[31] Z. Chen, Y. Wu, Y. Liu, S. Yang, Y. Chen, L. Lai, Discovery of dual target inhibitors against cyclooxygenases and leukotriene A4 hydrolase, J. Med. Chem. 54 (2011) 3650–3660. https://doi.org/10.1021/jm200063s.
[32] C. Yang, S. Chen, M. Zhou, Y. Li, Y. Li, Z. Zhang, Z. Liu, Q. Ba, J. Li, H. Wang, X. Yang, D. Ma, R. Wang, Development of 3-phenyl-N-(2-(3-phenylureido) ethyl)-thiophene-2-sulfonamide compounds as inhibitors of antiapoptotic bcl-2 family proteins, ChemMedChem 9 (2014) 1436–1452. https://doi.org/10.1002/cmdc.201400058.
[33] S. Liekens, S. Gijsbers, E. Vanstreels, D. Daelemans, E. De Clercq, S. Hatse, The nucleotide analog cidofovir suppresses basic fibroblast growth factor (FGF2) expression and signaling and induces apoptosis in FGF2-overexpressing endothelial cells, Mol. Pharmacol. 71 (2007) 695–703. https://doi.org/10.1124/mol.106.026559.
[34] J.M. Andreu, Tubulin purification, in: J. Zhou (Ed.), Methods in Molecular Medicine, Humana Press Inc, Totowa. NJ, 2007, pp. 17–28.
[35] C. Temple, G.A. Rener, R.N. Comber, New anticancer agents - alterations of the carbamate group of ethyl (5-amino-1,2-dihydro-3-phenylpyrido-3,4-*b*-pyrazin-7-yl)carbamates, J. Med. Chem. 32 (1989) 2363–2367. https://doi.org/10.1021/jm00130a023.
[36] M. Allan, S. Manku, E. Therrien, N. Nguyen, S. Styhler, M.-F. Robert, A.-C. Goulet, A.J. Petschner, G. Rahil, M.A. Robert, R. Deziel, J.M. Besterman,

H. Nguyen, A. Wahhab, N-Benzyl-1-heteroaryl-3-(trifluoromethyl)-1H-pyrazole-5-carboxamides as inhibitors of co-activator associated arginine methyltransferase 1 (CARM1), Bioorg. Med. Chem. Lett 19 (2009) 1218–1223. https://doi.org/10.1016/j.bmcl.2008.12.075.

[37] J.F. Diaz, R.M. Buey, Characterizing ligand-microtubule binding by competition methods, in: J. Zhou (Ed.), Methods in Molecular Medicine, Humana Press Inc., Totowa, NJ, 2007, pp. 245–260.

[38] P.J. Goodford, A computational procedure for determining energetically favorable binding sites on biologically important macromolecules, J. Med. Chem. 28 (1985) 849–857. https://doi.org/10.1021/jm00145a002.

[39] D.N.A. Boobbyer, P.J. Goodford, P.M. McWhinnie, R.C. Wade, New hydrogen-bond potentials for use in determining energetically favorable binding-sites on molecules of known structure, J. Med. Chem. 32 (1989) 1083–1094. https://doi.org/10.1021/jm00125a025.

[40] G.M. Morris, R. Huey, W. Lindstrom, M.F. Sanner, R.K. Belew, D.S. Goodsell, A.J. Olson, AutoDock4 and AutoDockTools4: automated docking with selective receptor flexibility, J. Comput. Chem. 30 (2009) 2785–2791. https://doi.org/10.1002/jcc.21256.